

RESEARCH ARTICLE

An improved representation of the relationship between photosynthesis and stomatal conductance leads to more stable estimation of conductance parameters and improves the goodness-of-fit across diverse data sets

Julien Lamour¹  | Kenneth J. Davidson^{1,2}  | Kim S. Ely¹  | Gilles Le Moguédec³  |
 Andrew D. B. Leakey^{4,5,6}  | Qianyu Li¹  | Shawn P. Serbin¹  | Alistair Rogers¹ 

¹Environmental & Climate Sciences Department, Brookhaven National Laboratory, Upton, New York, USA

²Department of Ecology and Evolution, Stony Brook University, Stony Brook, New York, USA

³AMAP, Université Montpellier, INRAE, Cirad CNRS, IRD, Montpellier, France

⁴Department of Plant Biology, University of Illinois at Urbana-Champaign, Urbana, Illinois, USA

⁵Department of Crop Sciences, University of Illinois at Urbana-Champaign, Urbana, Illinois, USA

⁶Carl R. Woese Institute for Genomic Biology, University of Illinois at Urbana-Champaign, Urbana, Illinois, USA

Correspondence

Julien Lamour, Environmental & Climate Sciences Department, Brookhaven National Laboratory, Upton, NY, USA.
 Email: jlamour.sci@gmail.com

Funding information

U.S. Department of Energy, Grant/Award Number: DE-SC0012704 and DE-SC0018277

Abstract

Stomata play a central role in surface–atmosphere exchange by controlling the flux of water and CO₂ between the leaf and the atmosphere. Representation of stomatal conductance (g_{sw}) is therefore an essential component of models that seek to simulate water and CO₂ exchange in plants and ecosystems. For given environmental conditions at the leaf surface (CO₂ concentration and vapor pressure deficit or relative humidity), models typically assume a linear relationship between g_{sw} and photosynthetic CO₂ assimilation (A). However, measurement of leaf-level g_{sw} response curves to changes in A are rare, particularly in the tropics, resulting in only limited data to evaluate this key assumption. Here, we measured the response of g_{sw} and A to irradiance in six tropical species at different leaf phenological stages. We showed that the relationship between g_{sw} and A was not linear, challenging the key assumption upon which optimality theory is based—that the marginal cost of water gain is constant. Our data showed that increasing A resulted in a small increase in g_{sw} at low irradiance, but a much larger increase at high irradiance. We reformulated the popular Unified Stomatal Optimization (USO) model to account for this phenomenon and to enable consistent estimation of the key conductance parameters g_0 and g_1 . Our modification of the USO model improved the goodness-of-fit and reduced bias, enabling robust estimation of conductance parameters at any irradiance. In addition, our modification revealed previously undetectable relationships between the stomatal slope parameter g_1 and other leaf traits. We also observed nonlinear behavior between A and g_{sw} in independent data sets that included data collected from attached and detached leaves, and from plants grown at elevated CO₂ concentration. We propose that this empirical modification of the USO model can improve the measurement of g_{sw} parameters and the estimation of plant and ecosystem-scale water and CO₂ fluxes.

KEYWORDS

leaf gas exchange, minimum conductance, optimality model, residual conductance, stomatal conductance, trait covariation, transpiration, water use efficiency

1 | INTRODUCTION

Stomata regulate the exchange of carbon dioxide (CO_2) and water vapor between leaves and the atmosphere (Buckley, 2019; Cowan & Farquhar, 1977). Mathematical representation of stomatal conductance is therefore essential to simulating the carbon, water and energy fluxes of leaves, plants and ecosystems (Sellers et al., 1997). Several approaches have been used to describe the relationship between stomatal conductance to water vapor (g_{sw}), photosynthesis (A), and environmental conditions at the leaf surface, that is, CO_2 concentration, relative humidity (RH) or leaf to air vapor pressure deficit (VPD_{leaf} ; Buckley & Mott, 2013; Damour et al., 2010). Many of these models have a similar structure related to the assumed linear relationship between the steady state values of g_{sw} and A for a given set of environmental conditions. Typically, models have two parameters, (1) the slope (g_1 , m , or k) of the relationship between g_{sw} and a regressor consisting of A and environmental conditions at the leaf surface and (2) g_0 , the value of g_{sw} when A is zero. A number of analyses have shown that although some model formulations perform better than others, the principal driver of model performance is not the model formulation but the parameterization of the slope parameter (hereafter g_1) and the intercept (g_0 ; Franks et al., 2017; Hérault et al., 2013; Körner, 1995; Lin et al., 2015; Wolz et al., 2017; Wu et al., 2020). Many model formulations also include additional empirical modification of the relationship between g_{sw} and A using a scaling factor related to leaf water potential or soil water potential that is used to adjust g_0 , g_1 or maximum carboxylation capacity (Anderegg et al., 2017; De Kauwe et al., 2015; Rogers et al., 2017; Tuzet et al., 2003).

The slope parameter g_1 is directly related to the marginal water cost of carbon gain (λ) also known as the inverse of the water use efficiency (WUE, $\text{WUE} = 1/\lambda$, Bonan et al., 2014). A leaf with a high g_1 will lose more water per mol of CO_2 assimilated than a leaf with a low g_1 . Previously, terrestrial biosphere models (TBMs) accounted for variation in g_1 between plants with the C3 or C4 photosynthetic pathways (De Kauwe et al., 2015; Franks et al., 2018). However, leaf-level analyses of stomatal behavior have demonstrated that g_1 varies significantly at various organizational scales, including variation among biomes, plant functional types, and species (Franks et al., 2017, 2018; Lin et al., 2015; Wolz et al., 2017). Parameterization of stomatal models to capture this variation offers a path for improved model representation of g_{sw} in TBMs. Accounting for variation in g_1 has also been shown to be important for modelling g_{sw} within a single species (Ono et al., 2013; Zhu et al., 2011), but with inconsistent results in other studies (Miner & Bauerle, 2017). Overall, the drivers of variability in the g_1 parameter are still poorly understood and, there has only been evidence of weak correlations with a limited number of leaf traits, and limited information on its plasticity or acclimation (Franks et al., 2018; Rogers et al., 2017; Wu et al., 2020). Improved understanding of leaf trait covariance, and environmental drivers of the variation in the g_1 parameter would be useful to better inform model parameterization of g_1 .

The intercept parameter g_0 represents conductance when photosynthesis is zero with different meanings depending upon the conductance model considered. From a biological perspective, it is widely accepted that conductance reaches its minimum value in the dark ($g_{\text{sw,dark}}$) but is always positive (Duursma et al., 2019; Yu et al., 2019). This may be attributable to cuticular conductance or diffusion through incompletely closed stomata (Boyer et al., 1997; Machado et al., 2021; Márquez et al., 2021; Saito & Futakuchi, 2010). In conductance models where gross photosynthesis (A_g) is used to model the effect of A on g_{sw} (e.g., Yin & Struik, 2009), g_0 mathematically corresponds to $g_{\text{sw,dark}}$ ($g_0 = g_{\text{sw,dark}}$) and is independent from other variables at the leaf surface. In models where the net photosynthesis (A_n) is the response variable (e.g., Medlyn et al., 2011; Tuzet et al., 2003), $g_{\text{sw,dark}}$ is mathematically lower than g_0 and corresponds to the value of g_{sw} for A_n in the dark, that is, when A_n is equal to the rate of dark respiration (R_{dark}). In those formulations, $g_{\text{sw,dark}}$ can be negative because it depends on g_1 , g_0 , R_{dark} , and the conditions at the leaf surface (Yin & Struik, 2009). To compensate for this issue TBMs that use an A_n type conductance model add a constraint that limits $g_{\text{sw,dark}}$ whereby $g_{\text{sw,dark}} = g_0$ and all the values below g_0 are, therefore, fixed at g_0 (De Kauwe et al., 2015; Lombardozzi et al., 2017). Importantly, this constraint makes the relationship between g_{sw} and A_n nonlinear, and not continuous around the light compensation point with a zero slope for irradiance levels below the light compensation point, and a positive slope, equal to g_1 above it.

An important consideration for most conductance models is their dependence on the variable A (A_n or A_g), that in contrast to the other variables of the model (CO_2 , RH, or VPD_{leaf}), is not an environmental variable but a physiological one. A depends, in part, on environmental variables such as irradiance, CO_2 concentration, and temperature, and any change in the environmental conditions that affect A will also affect g_{sw} . Therefore, models of g_{sw} are necessarily coupled to a model of A to be able to simulate g_{sw} in various environmental conditions. As a consequence, in addition to the parameters g_0 and g_1 , g_{sw} also depends on the parameters associated with A , such as R_{dark} (which determines $g_{\text{sw,dark}}$) and the photosynthetic capacity, which determines the maximum A and maximum g_{sw} . In fact, previous work has shown that variation in photosynthetic capacity is a key driver of variation in seasonal and leaf age dependent g_{sw} (Chen et al., 2019; Xu & Baldocchi, 2003; Zhou et al., 2013).

Importantly, previous work has described a nonlinearity between A and g_{sw} at low irradiance (Ball, 1988; Barnard & Bauerle, 2013). However, its effect on the representation of g_{sw} remains a critical knowledge gap, and the irradiance at which nonlinearity is apparent is still unclear. Ball (1988) reported that it was most consistently visible below $150 \mu\text{mol m}^{-2} \text{s}^{-1}$ but that the irradiance at which the relationship became nonlinear varied. It is important to note that the light compensation point is typically much lower than $150 \mu\text{mol m}^{-2} \text{s}^{-1}$ for most plants (Craine & Reich, 2005; Sterck et al., 2013) and that at $150 \mu\text{mol m}^{-2} \text{s}^{-1}$ notable rates of A are observed in many species. Understanding the relationship between g_{sw} and A is important because if the relationship is not linear, g_1 is not constant across the range of A . This would impact the estimation of g_1 under

TABLE 1 Description of the species of the study

Species name	Leaf lifetime (days)	Leaf size (width × length, cm)	Shade tolerance	Life form	Foliage
<i>Brosimum utile</i> (Kunth) Oken	324	6 × 11	Shade tolerant	Tree	Evergreen
<i>Cecropia insignis</i> Liebm.	231	47 × 48	Light demanding	Tree	Evergreen
<i>Gutteria dumetorum</i> R.E. Fr.	212	3.5 × 9	Light demanding	Tree	Evergreen
<i>Miconia minutiflora</i> (Bonpl.) DC.	189	5 × 11	Light demanding	Shrub	Evergreen
<i>Terminalia amazonia</i> (J.F. Gmel.) Exell	160	4 × 9	Light demanding	Tree	Brevideciduous
<i>Vochysia ferruginea</i> Mart.	215	3.5 × 9	Shade tolerant	Tree	Evergreen

Note: The leaf lifetime and leaf size data were reported previously (Osnas et al., 2018).

different environmental conditions and bias the comparison of g_1 between leaves with different photosynthetic properties. These biases and uncertainties in g_1 would also impact ecosystem-scale simulations of carbon and water cycling (Dietze et al., 2014; Migliavacca et al., 2021).

Examination of the response of g_{sw} to environmental changes at the leaf surface have been undertaken in the tropics (Domingues et al., 2014; Fauset et al., 2019; Ghimire et al., 2018; Motzer et al., 2005; Wu et al., 2020). However, most of these studies were made using the survey measurement approach that relies on many rapid measurements of leaf gas exchange, typically made on multiple different leaves and under a range of environmental conditions. This approach assumes that measured A and g_{sw} are at steady state at the time of measurement and fully acclimated to the prevailing measurement conditions. The parameter g_1 can be estimated using this approach, but the estimation of g_0 can be more uncertain, particularly if the data set does not include measurements made at low irradiance (Duursma et al., 2019; Miner et al., 2017). This approach is not suitable to study the response of leaves to gradients of environmental conditions as measurements are usually not repeated on the same leaves. The alternative approach is a response curve where steady-state measurements of g_{sw} are made along a gradient of environmental conditions, set, and controlled by the gas exchange instrument. In the tropics, we found only one study that used a steady-state response curve approach to study the effect of VPD_{leaf} on g_{sw} (Domingues et al., 2014). To our knowledge, the response of g_{sw} to A has never been studied in detail in tropical forests despite the central role of stomata in regulating the water vapor and CO_2 fluxes in this globally important biome.

This study aimed to investigate the relationship between A and g_{sw} and determine if the potential non-linearity of this relationship should be represented in leaf and ecosystem-scale models. Therefore, the objectives of the study were to understand the strength of the nonlinearity, its effects on the ability to robustly estimate g_0 and g_1 and the impact of nonlinearity on the prediction of CO_2 and water vapor fluxes. To address these objectives, we measured the steady state g_{sw} response to modification of the incident irradiance on tropical tree species with divergent ecological strategies, spanning a variety of leaf phenological stages. We also measured dark-adapted R_{dark} to enable estimation of $g_{sw,dark}$. We used the Unified Stomatal Optimization (USO) model (Medlyn et al., 2011)

as a foundation for our study since the model has a strong mathematical similarity with previous empirical models (Ball et al., 1987; Leuning, 1995), a solid theoretical background (Medlyn et al., 2011) and uses vapor pressure deficit rather than relative humidity (Rogers et al., 2017). We tested two additional model formulations to evaluate if they could provide an improved estimation of g_0 and g_1 and a consequent improved goodness-of-fit of g_{sw} . In addition to evaluating the new formulations using our tropical data we also used three other independent data sets to test the generalizability of the new formulations on data acquired in attached versus detached leaves (Davidson et al., 2022), ambient versus elevated CO_2 concentration (Leakey et al., 2006) and on the large global conductance data set from Lin et al. (2015), which included survey conductance measurements collected from multiple biomes and species. Finally, we also compared the predictions of water vapor and CO_2 fluxes among the different stomatal model formulations by using a leaf-level model of gas exchange that is commonly implemented in TBMs.

2 | MATERIALS AND METHODS

2.1 | Panama study site and plant material

The primary study site was located in the protected area of San Lorenzo Forest, in Colón Province, in the Republic of Panama (9.280°N, -79.975°W, 120 m above sea level) and has been described in detail previously (Basset, 2003; Slot & Winter, 2017; Wu et al., 2020). This forest has not experienced anthropogenic disturbance for more than 150 years (Basset, 2003). The climate is tropical and characterized by low variation around a mean temperature of about 25°C. The rainy season spans from May to December with monthly precipitation around 370 mm. The rest of the year is much drier with monthly precipitation around 80 mm. The measurement campaign was during January to March 2020, during the dry season.

Leaves from different species and at different leaf phenological stages were selected to have a diversity of leaf material with respect to their traits (Table 1; Osnas et al., 2018), photosynthetic rates and conductance, and an anticipated variety of g_0 and g_1 parameters. A 52-m canopy crane with a 54-m jig enabled access to the top of the canopy, averaging 26 m above ground, of the six tropical tree species we investigated (Table 1). Four species; *Gutteria dumetorum*

R.E. Fr., *Miconia minutiflora* (Bonpl.) DC., *Terminalia amazonia* (J.F. Gmel.) Exell, and *Vochysia ferruginea* Mart. had been studied previously (Wu et al., 2020) and had shown a range of g_1 values associated with mature leaves. For this study two additional contrasting species *Brosimum utile* (Kunth) Oken and *Cecropia insignis* Liebm. were added and for all six species several leaves at three stages of development; young ($n = 2 - 5$), mature ($n = 4 - 7$), and old ($n = 3 - 5$) were measured. The leaf stage of development was identified visually, the young leaves being often lighter green and at the tip of the branches, the old leaves being further down the branches, thicker, and often darker (Wu et al., 2017).

Using the canopy crane, branches from the top of the canopy were removed before dawn, placed into buckets filled with water and recut following established methods necessary to avoid xylem cavitation (Sperry, 2013; Wu et al., 2020). Such an approach has been demonstrated to successfully yield parameter estimates that correspond well with independent measurements of leaf gas exchange in situ (Leakey et al., 2006; Wolz et al., 2017). The branches were placed in a shaded area where the gas exchange measurements were made.

2.2 | Leaf gas exchange measurements

The response of g_{sw} to irradiance was used to estimate g_1 and g_0 . The approach required measurement of steady state g_{sw} to decreasing irradiance and has been described previously (Ball et al., 1987; Kromdijk et al., 2019; Leakey et al., 2006; Wolz et al., 2017). We used this “response curve” approach rather than survey measurements (e.g., Wu et al., 2020) to measure in detail the response of conductance to changes in photosynthesis at the leaf scale.

Five LI-6400XT portable infrared gas analyzers equipped with a $2 \times 3 \text{ cm}^2$ leaf chamber and red-blue light source (90% red, 10% blue) and one LI-6800 Portable Photosynthesis System (LI-COR) equipped with Multiphase Flash Fluorometer leaf chamber (6800-01A) were used for the measurements.

The response of g_{sw} to irradiance was measured by sequentially lowering the irradiance and included a measurement with the light source off ($0 \mu\text{mol m}^{-2} \text{ s}^{-1}$). For all the species except *M. minutifolia*, irradiance varied from 1000 to $0 \mu\text{mol m}^{-2} \text{ s}^{-1}$. For *M. minutifolia*, which had a higher light saturation point, irradiance varied from 1500 to $0 \mu\text{mol m}^{-2} \text{ s}^{-1}$. When performing the last measurement of the response curve at 0 irradiance, a dark cloth was placed over the measured branch to prevent sunlight from diffusing inside the cuvette. This constituted the dark-adapted measurement of the leaves. The time interval between each light level was manually adjusted so that A and g_{sw} were visually stable and varied between 10 and 45 min.

Leaf temperature (T_{leaf}) was controlled by the instrument for the duration of each response curve (SD of 0.1°C for a given curve) and was set between 28 and 32°C depending on prevailing environmental conditions. The CO_2 concentration in the leaf chamber was controlled and set to 400 ppm. The humidity inside the leaf chamber

fluctuated with ambient conditions but was controlled using a combination of the T_{leaf} set point and desiccant flow rate to avoid condensation inside the instrument. As a result of the humidity and temperature control, the average leaf to air vapor pressure deficit (VPD_{leaf}) was 1.2 kPa (SD of 0.11 for a given curve).

The instruments automatically logged points every 10 s, and the devices were set to automatically match the sample and reference infrared gas analyzers every 10 min. For each irradiance level, an average of the 5 log points prior to a change in irradiance constituted that measurement. The dark-adapted measurement of CO_2 and water vapor flux provided the estimation of R_{dark} and $g_{sw,dark}$. The A measured at the first saturating irradiance provided estimation of the light-saturated CO_2 assimilation rate (A_{sat}).

2.3 | Estimation of maximum carboxylation capacity

For our leaf-level modeling, we required an estimate of maximum carboxylation capacity. We used the “one-point method” (De Kauwe et al., 2016) to estimate the maximum rate of carboxylation (V_{cmax}) of each leaf. Robust measurement for determination of V_{cmax} using the one-point method requires a measurement of steady-state A_{sat} and the corresponding intracellular CO_2 concentration as input variables (Burnett et al., 2019). The V_{cmax} at measurement temperature was then scaled to the reference temperature of 25°C (V_{cmax25}) using a modified Arrhenius equation with the parameters for tropical species growing at a mean ambient temperature of 25°C (Kumarathunge et al., 2019).

2.4 | Leaf structural and nitrogen trait measurements

The leaf mass per unit leaf area (LMA) and leaf nitrogen concentration per unit leaf area (N_a) were measured after the completion of the conductance curves. Discs of known area were extracted from different places on the leaves, avoiding large veins and the mid-rib. They were then dried at 70°C for several days to achieve constant mass and weighed to calculate the LMA . Dried leaves were subsequently ground, and elemental nitrogen was quantified using a 2400 Series II CHN analyzer following the manufacturer's instructions (PerkinElmer).

2.5 | Conductance models

Four model formulations based on the USO model (Medlyn et al., 2011) were used to represent the response of g_{sw} to irradiance.

The first model is the original, full USO model (Equation 1, hereafter USO_{full}) that was derived mathematically.

$$g_{sw} = g_0 + 1.6 \left(1 + \frac{g_1}{\sqrt{VPD_{leaf}}} \right) \frac{A_n}{CO_{2s}}, \quad (1)$$

where g_0 is the g_{sw} when A_n equals 0, g_1 the slope parameter which is proportional to the water cost of carbon gain (Medlyn et al., 2011), VPD_{leaf} the leaf to air vapor pressure deficit, A_n the net assimilation and CO_{2s} the concentration of CO_2 at the leaf surface.

The second model (Equation 2, hereafter USO) is an approximation of the mathematically derived USO_{full} model and is analogous to the empirical models from Ball et al. (1987) and Leuning (1995) (Medlyn et al., 2011). The USO model was evaluated here for comparison with the original full model to be sure that differences between the USO_{full} and USO models do not arise from this simplification.

$$g_{sw} = g_0 + 1.6 \frac{g_1}{\sqrt{VPD_{leaf}}} \frac{A_n}{CO_{2s}}. \quad (2)$$

In both the USO and USO_{full} formulations $g_{sw,dark}$ is dependent on g_1 , R_{dark} , CO_{2s} , and VPD_{leaf} (Table 2).

Following previous work (Yin & Struik, 2009) an alternative g_{sw} formulation was introduced that uses A_g , that is, $A_n + R_{dark}$, to ensure g_{sw} is always positive and greater than g_0 (Equation 3, hereafter USO_{A_g})

$$g_{sw} = g_0 + 1.6 \frac{g_1}{\sqrt{VPD_{leaf}}} \frac{A_g}{CO_{2s}}. \quad (3)$$

Note that for the USO_{A_g} formulation, $g_0 = g_{sw,dark}$ (Table 2).

Finally, we considered a new empirical g_{sw} formulation where the effect of A_g on g_{sw} was squared and therefore nonlinear (Equation 4, hereafter $USO_{A_g^2}$). This formulation differs from most commonly used g_{sw} models for which the effect of A on g_{sw} is linear (Damour et al., 2010).

$$g_{sw} = g_0 + 1.6 \frac{g_1}{\sqrt{VPD_{leaf}}} \frac{A_g^2}{CO_{2s}}. \quad (4)$$

In the $USO_{A_g^2}$ formulation, g_0 equals $g_{sw,dark}$ (Table 2). Note that for the USO_{A_g} and $USO_{A_g^2}$ formulations, $g_{sw,dark}$ can be measured directly with a dark-adapted measurement of leaf gas exchange. However, when using the USO_{full} or USO formulations a direct measurement of $g_{sw,dark}$ would require a priori knowledge of the light compensation point.

TABLE 2 The different conductance models rearranged in the linear form $Y = g_0 + g_1X$

Conductance model	Y	X	Predicted g_{sw}	Predicted $g_{sw,dark}$
USO_{full} (Equation 1)	$g_{sw} - \frac{1.6A_n}{CO_{2s}}$	$\frac{1.6A_n}{CO_{2s}\sqrt{VPD_{leaf}}}$	$g_0 + g_1X + \frac{1.6A_n}{CO_{2s}}$	$g_0 - 1.6 \left(1 + \frac{g_1}{\sqrt{VPD_{leaf}}}\right) \frac{R_{dark}}{CO_{2s}}$
USO (Equation 2)	g_{sw}	$\frac{1.6A_n}{CO_{2s}\sqrt{VPD_{leaf}}}$	$g_0 + g_1X$	$g_0 - \frac{1.6g_1}{\sqrt{VPD_{leaf}}} \frac{R_{dark}}{CO_{2s}}$
USO_{A_g} (Equation 3)	g_{sw}	$\frac{1.6A_g}{CO_{2s}\sqrt{VPD_{leaf}}}$	$g_0 + g_1X$	g_0
$USO_{A_g^2}$ (Equation 4)	g_{sw}	$\frac{1.6A_g^2}{CO_{2s}\sqrt{VPD_{leaf}}}$	$g_0 + g_1X$	g_0

Note: In the four models, g_0 is expressed in $\text{mol m}^{-2} \text{s}^{-1}$. g_1 is expressed in $\text{kPa}^{0.5}$ in the USO_{full} , USO and USO_{A_g} models but is expressed in $\mu\text{mol}^{-1} \text{m}^2 \text{s kPa}^{0.5}$ in the $USO_{A_g^2}$ model.

2.6 | Fitting conductance models

Fitting of the models to estimate g_0 and g_1 was completed at the leaf scale, using the data from each leaf individually. The parameters g_0 and g_1 were estimated using linear regression. Each model formulation was rearranged into the linear form $Y = g_0 + g_1X$ (Table 2), where X is considered as the regressor and Y the response variable, which corresponds to g_{sw} for all the models except USO_{full} (Table 2). For the USO_{full} model, g_{sw} was not equal to Y so its calculation is also presented in Table 2. The goodness-of-fit of g_{sw} was evaluated by comparison of the RMSE and R^2 of the modeled versus observed conductance for each formulation.

2.7 | Test of the linearity assumption

The USO_{full} , USO, and USO_{A_g} models (Equations 1 and 2) assume that the effect of A on g_{sw} is linear. We tested if this assumption was valid by evaluating the response of leaf level conductance to irradiance by comparing Y with X and by assessing if the slope (g_1) of the relationship was constant. To do this, we analyzed the residuals (ϵ , Equation 5) of each linear regression for each model (Equations 1 to 4) to evaluate whether the assumption of linearity between Y and X holds.

$$\epsilon = Y_{obs} - Y_{pred}. \quad (5)$$

The residuals should have a normal distribution with a zero mean and without a trend. To test if a trend was present and as it is classically done in diagnostics of linear regressions, we fitted a nonparametric smoothing function (LOESS) to the residuals for different Y ordinates. Following our nomenclature in Table 2, the residuals for the linear regressions associated with each model are denoted as, ϵ_{full} , ϵ , ϵ_{A_g} and $\epsilon_{A_g^2}$.

2.8 | Effect of the irradiance levels used in the estimation of g_0 and g_1

A test was performed to assess the effect of the range in A upon estimation of g_0 and g_1 . Initially, all the points were considered to estimate g_0 and g_1 . Secondly, only the points measured with an

irradiance above the light compensation point ($A_n = 0$) of each leaf were considered. Finally, following Ball (1988), we considered only the data acquired at an irradiance greater than $150 \mu\text{mol m}^{-2} \text{s}^{-1}$. For each model, we compared g_0 and g_1 estimated with these three scenarios using a student's *t*-test ($n = 78$ independent response curves).

2.9 | Leaf trait correlation with g_0 and g_1 estimated by the different models and performance of estimation of $g_{\text{sw, dark}}$

We evaluated if the variation in the parameter g_1 estimated by the different models could be explained by species or leaf phenological stage. We evaluated this using an analysis of variance (ANOVA) with the leaf phenological stage and the species as fixed effects and compared the coefficient of determination R^2 for the different conductance models. We also tested if g_1 was correlated with different leaf traits ($V_{\text{cmax}25}$, $R_{\text{dark}25}$, LMA and N_a) using a Pearson correlation test. We performed the same analysis for g_0 . Finally, we assessed the goodness-of-fit of $g_{\text{sw, dark}}$ using the different conductance models (Table 2).

2.10 | Comparison of the performance of the USO and $\text{USO}_{A_g^2}$ on independent data sets

The performance of the USO and $\text{USO}_{A_g^2}$ models were evaluated on three independent data sets; a response curve experiment on hybrid poplar with intact in situ measurements and parallel ex situ measurements on detached branches (Davidson et al., 2022), a response curve data set from Leakey et al. (2006), and a survey data set from Lin et al. (2015).

First, we used data acquired on 2-year-old poplar (*Populus deltoides*) grown outside in pots at Brookhaven National Laboratory, Upton, New York (40.8656°N, 72.8814°W, 18 m above sea level). This experiment was conducted to evaluate the effect of excising a branch on the measurement of stomatal response curves. To this end, we measured the steady-state response of g_{sw} to irradiance on branches attached to the plant and on excised branches following our Panama protocol. The VPD_{leaf} was also better controlled and remained strictly constant during the curves. More details can be found in Davidson et al. (2022).

Secondly, we used the Leakey et al. (2006) data set, which was collected at the SoyFACE facility in Champaign (40.033°N, 88.230°W, 228 m above sea level) on soybean exposed to current ($378 \mu\text{mol mol}^{-1}$) and elevated ($552 \mu\text{mol mol}^{-1}$) CO_2 concentration in a free-air CO_2 enrichment experiment conducted in 2003. The conductance measurements were made on excised leaves and consisted of conductance response curves. On each leaf, the conductance response curves included a first phase where $\text{CO}_{2\text{s}}$ was modified (values between 50 and $1500 \mu\text{mol mol}^{-1}$) while keeping VPD_{leaf} below 1 kPa and the irradiance constant at $1500 \mu\text{mol m}^{-2} \text{s}^{-1}$, and a second phase where the irradiance was modified from 1500 to $0 \mu\text{mol m}^{-2} \text{s}^{-1}$ while keeping the $\text{CO}_{2\text{s}}$ constant at 370 or 550 ppm with a constant VPD_{leaf} below 1 kPa.

Data below 400 ppm $\text{CO}_{2\text{s}}$ were not used in model parametrization as the USO model was not built to represent rubisco limited photosynthesis (Medlyn et al., 2011). This data set was complementary to our data set since it also included variation in $\text{CO}_{2\text{s}}$ and allowed us to test if the new conductance model we proposed, $\text{USO}_{A_g^2}$, would also be suitable to model g_{sw} at elevated CO_2 concentration.

Finally, we compared the goodness-of-fit of the USO and $\text{USO}_{A_g^2}$ conductance models on the Lin et al. (2015) data set—the largest publicly available data set for assessing stomatal model formulations. This data set is comprised of survey measurements made by different researchers in 56 different field studies and included a wide variety of leaf surface conditions (95% of VPD_{leaf} was between 0.6 and 6 kPa, T_{leaf} between 5 and 45°C) at ambient CO_2 levels (95% of CO_2 concentration at the leaf surface were between 304 and $410 \mu\text{mol mol}^{-1}$). This data set allowed us to test whether the $\text{USO}_{A_g^2}$ model was suitable for modeling g_{sw} in a wide variation of VPD_{leaf} and T_{leaf} . This data set only included measurement made for positive values of A_n , at irradiance levels above the light compensation point. In addition, the Lin et al. (2015) data did not include measurements of R_{dark} . To enable calculation of A_g we used a value of R_{dark} estimated from the mean global leaf respiration rate and the associated temperature response (Heskel et al., 2016; Equation 6).

$$\ln(R_{\text{dark}}) = -2.2276 + 0.1012T_{\text{leaf}} - 0.0005T_{\text{leaf}}^2 \quad (6)$$

2.11 | Impact of the conductance models on leaf scale gas exchange simulations

To evaluate the effect of using the USO or $\text{USO}_{A_g^2}$ conductance models to calibrate g_0 and g_1 and to simulate g_{sw} we performed simulations of the response of g_{sw} and A to irradiance in R (R Core Team, 2020) using the package LeafGasExchange (Lamour & Serbin, 2021). This package simulated photosynthesis using the Farquhar et al. (1980) model, which we coupled with the USO and $\text{USO}_{A_g^2}$ conductance models. Note that the use of a coupled model of photosynthesis and conductance is typically used in TBMs (Bonan et al., 2011; Clark et al., 2011; Krinner et al., 2005; Rogers et al., 2017). The analytical solution of the system of equations used to couple the photosynthesis and conductance models for the new formulation $\text{USO}_{A_g^2}$ is given in the Appendix. We parametrized the model for an average leaf using the average g_0 and g_1 obtained by either the USO or $\text{USO}_{A_g^2}$ conductance models (Figure 3, All irradiances), the average $V_{\text{cmax}25}$ estimated by the one-point method and the average $R_{\text{dark}25}$. The $J_{\text{max}25}$ was modeled using a fixed ratio to $V_{\text{cmax}25}$ ($J_{\text{max}25} = 1.67V_{\text{cmax}25}$; Medlyn et al., 2002). The fixed parameters used to describe photosynthesis were the standard for C3 species (Lamour & Serbin, 2021). The input variables we used to perform the simulations were held constant and were the values measured during our field campaign, except for the irradiance which varied between 0 and $2000 \mu\text{mol m}^{-2} \text{s}^{-1}$ ($T_{\text{leaf}} = 30.1^\circ\text{C}$, $VPD_{\text{leaf}} = 1.2$ kPa, $\text{CO}_{2\text{s}} = 400$ ppm).

3 | RESULTS

3.1 | Test of the assumption of linearity between g_{sw} and A

Over the range of irradiance used in our experiment it is clear that the relationship of the response variable (Y axis, Table 2) to the model regressor (X axis, Table 2) in the full USO model formulation (USO_{full}) is not linear (Figure 1a and Figure S1). At low A (low X ordinates), the slope of the relationship between Y and X is shallow or even flat relative to the slope with median values of A , and at high A

(high X ordinates) the slope was steeper than the slope over median A values. This is also supported by the analysis of the residuals of the regression (USO_{full} , Figure 2a). A strong trend was present with a deviation between -0.01 and $0.05 \text{ mol m}^{-2} \text{ s}^{-1}$ from the expected mean of $0 \text{ mol m}^{-2} \text{ s}^{-1}$ and with an overestimation of the residuals for low and high Y values. When the USO_{full} model is simplified to approximate common empirical models (USO) the response of g_{sw} to the regressor is visually identical to the USO_{full} model, and the nonlinearity is still readily apparent (Figures 1b and 2b) indicating that nonlinearity in the USO formulation was not the result of simplification of the USO_{full} formulation. The mean R^2 and RMSE were

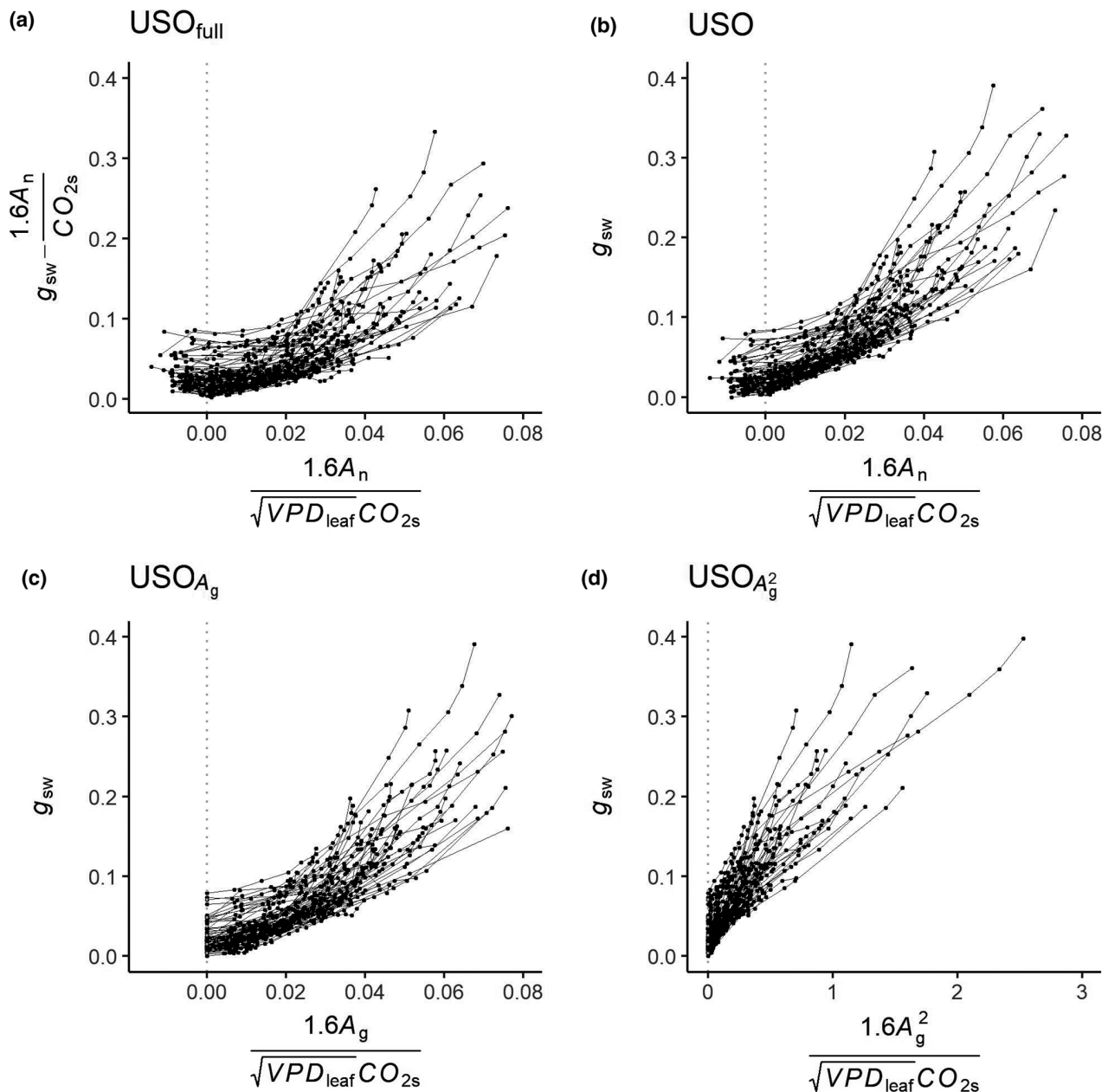


FIGURE 1 Representation of the conductance response curves to modification of the irradiance measured on leaves at different phenological ages (young, mature, old) from six tropical species. Each line represents the conductance response curve of one leaf and each point represents the measurements at the different irradiances. The x axis and the y axis correspond to the variables X and Y in Table 2 for different conductance models, with, in (a) the full USO model (USO_{full} , Equation 1), (b) the simplified USO model (USO, Equation 2), (c) the new formulation of the simplified USO model with A_g instead of A (USO_{A_g} , Equation 3) and (d) the new formulation with A_g^2 instead of A_n ($USO_{A_g^2}$, Equation 4). Note that the x and y axis have the same scale in the different panels, except for the x axis of the model $USO_{A_g^2}$ (panel d)

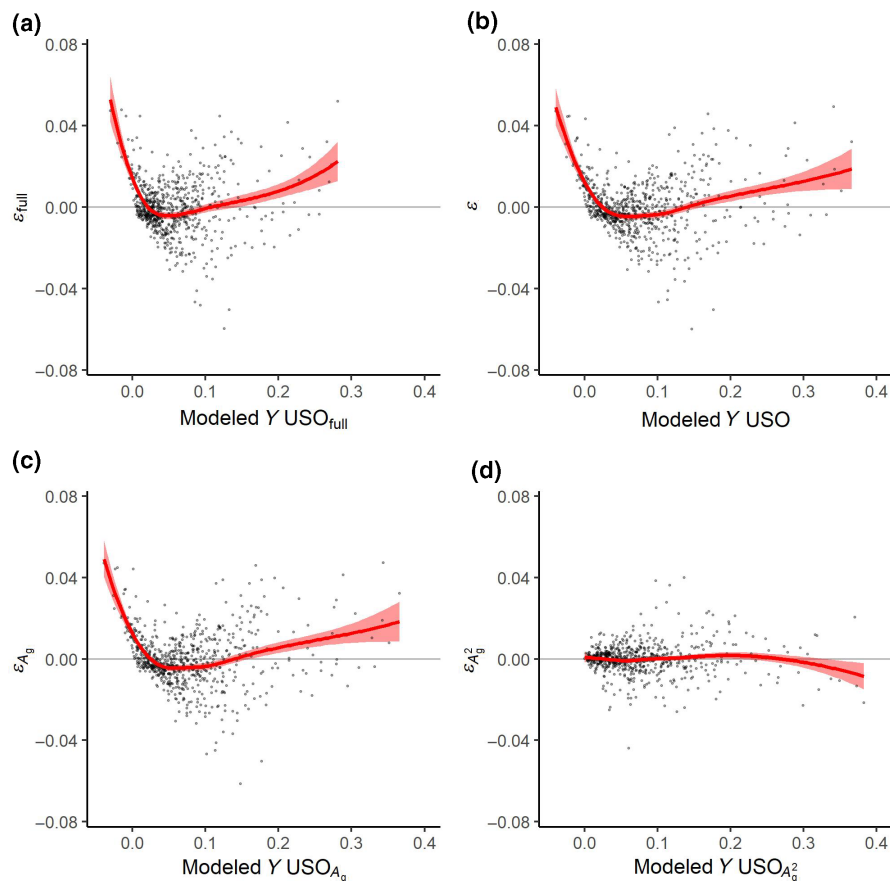


FIGURE 2 Representation of the residuals (ε) of the regression between the response variable Y and the regressor X (Table 2) for each conductance models USO_{full} , USO , USO_{A_g} , and $USO_{A_g^2}$. The red line presents the trend of the residuals and the shaded area represents the standard error of the mean [Colour figure can be viewed at wileyonlinelibrary.com]

the same for the USO_{full} and USO models ($R^2 = .91$, $RMSE = 0.013$, Figure 3). Note that for the USO_{full} and USO formations the lowest X ordinate was always negative due to the use of A_n (Figure 1a,b). In the formulations that used A_g (USO_{A_g} and $USO_{A_g^2}$, Figure 1c,d) the lowest X ordinate was always zero. Use of A_g in place of A_n (USO_{A_g}) did not improve the ability of the model to describe the data ($R^2 = .91$, $RMSE = 0.013$, Figure 3). Moreover, the nonlinearity was still evident as seen in Figures 1c and 2c. Our new model formulation in which the A_g term is squared ($USO_{A_g^2}$) resulted in a linear model fit with a better goodness-of-fit ($R^2 = .97$) and a 50% lower RMSE than the other formulations (Figures 1d, 2d and 3d).

3.2 | Consequence of the nonlinearity on the estimation of g_0 and g_1

Estimates of g_0 and g_1 by the USO_{full} , USO , and USO_{A_g} model formulations were affected by the range of irradiance over which data were collected (Figure 3). Despite being markedly lower than saturating irradiance, the irradiance value of $150 \mu\text{mol m}^{-2} \text{s}^{-1}$ corresponded to a measured A_n and g_{sw} that were nearly 40% of the light saturated values. When data were restricted to irradiances above this threshold, estimates of g_1 were 40%–70% higher when compared to estimates derived from the entire data set. In the same manner, g_0 decreased and always became negative. When using the $USO_{A_g^2}$

model, the parameters g_0 and g_1 remained statistically identical across the full range of irradiance. This showed that estimating the conductance parameters with $USO_{A_g^2}$ was more robust and less dependent on the environmental conditions during the measurement. Moreover, the analysis of the residuals of the USO_{full} , USO and USO_{A_g} models still showed a curvilinear trend when the range of irradiance was limited to data collected above $150 \mu\text{mol m}^{-2} \text{s}^{-1}$ (Figure 4). This trend was absent in the $USO_{A_g^2}$ model and the RMSE of this model was always the lowest (Figure 3).

3.3 | Comparison of the regression coefficients g_0 and g_1 obtained with the different model formulations

The different formulations affected the derived regression coefficients (Figures 3, 5, and 6). The full and simplified versions of the USO model (USO_{full} and USO) gave very similar values for g_0 (Figure 5a) but different values for g_1 with an intercept slightly above 1 (Figure 6a). The g_1 estimations were, however, highly correlated ($R^2 = .99$). Changing the formulation to use A_g in place of A_n (USO_{A_g}) changed the estimation of g_0 but did not change the estimation of g_1 (Figures 5b and 6b). However, estimations of g_1 made using the $USO_{A_g^2}$ model were markedly different from the one made using the

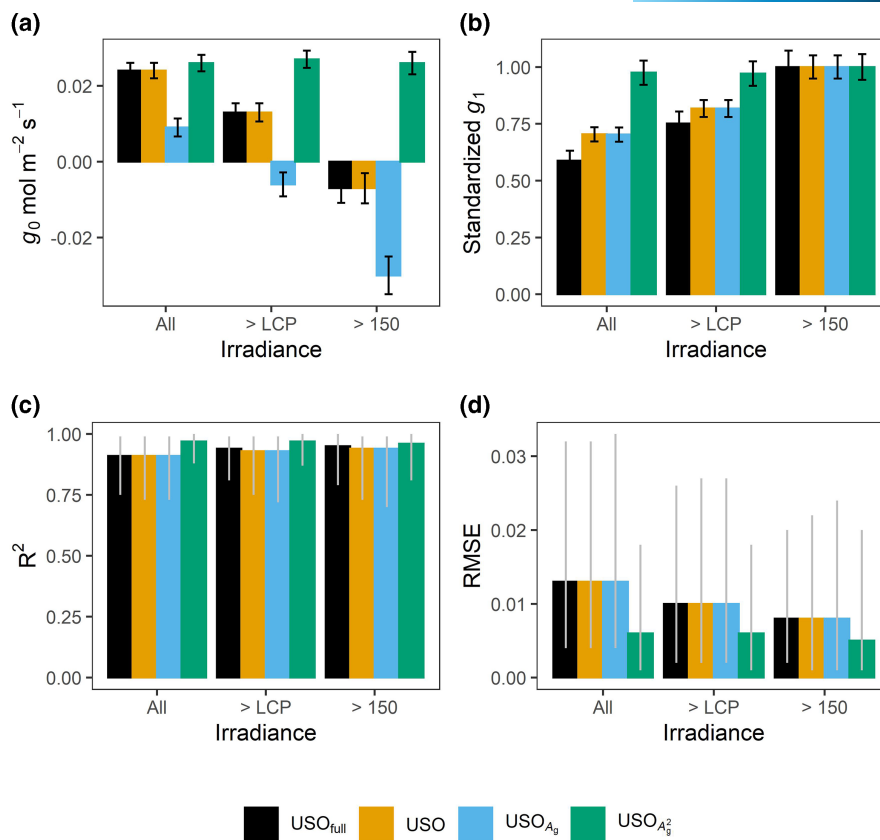


FIGURE 3 Estimated parameters g_0 and g_1 and performance of the different conductance models for different ranges of irradiance used for the regressions. (a) Intercept parameter g_0 . (b) Slope parameter g_1 . Because the value for g_1 is different for different formulations, their value is divided by their value estimated with the irradiance level above 150 $\mu\text{mol m}^{-2} \text{s}^{-1}$, i.e., 2.69, 3.78, 3.77 and 0.239 for the USO_{full}, USO, USO_{A_g} and USO_{A_g²} models, respectively. (c) Coefficient of determination R^2 . (d) Root Mean Square Error, RMSE. The error bars in black correspond to the 95% confidence interval of the mean g_0 and g_1 . The error bars in gray correspond to the 95% percentile of the calculated RMSE and R^2 which had a clear asymmetrical distribution. The statistics are obtained for 78 independent irradiance response curves. This figure demonstrates the strong effect of the irradiance range used for the regression for estimation of g_0 and g_1 with the USO_{full}, USO, and USO_{A_g} conductance models. The irradiance range did not have an effect on their estimation with the USO_{A_g²} model [Colour figure can be viewed at wileyonlinelibrary.com]

USO model (Figure 6c) and the coefficient of determination R^2 between the g_1 estimates was only .43 reflecting the different model structure. In Figures 5d and 6d, the result of considering USO_{A_g²} or USO_{A_n} (corresponding to Equation 4 but with A_n instead of A_g) on g_0 and g_1 are also shown. Considering A_n^2 in place of A_g^2 created a bias in both g_0 and g_1 estimates.

3.4 | Leaf trait correlation with g_0 and g_1 estimated by the different conductance models

The proportion of variation explained by the species and leaf phenological stage factors on g_1 was higher when it was estimated with the USO_{A_g²} model than with the other models (R^2 USO_{full} = .40, R^2 USO = .41, R^2 USO_{A_g} = .42, R^2 USO_{A_g²} = .63, Table 3). Similarly, g_1 estimated with the USO_{A_g²} model was correlated with $V_{\text{cmax}25}$, $R_{\text{dark}25}$ and N_a whereas the correlation was never significant for the other models (Table 4, Figure 7). The same analysis was performed for g_0 but its variation was very

poorly explained by the leaf phenological stage, species or the other leaf traits for all model formulations (Tables 3 and 4).

3.5 | Goodness-of-fit of $g_{\text{sw,dark}}$ by the different models

The goodness-of-fit of $g_{\text{sw,dark}}$ (Table 2) was compared for each model formulation (Figure 8). Comparisons among the USO_{full} (Figure 8a), USO (Figure 8b), and USO_{A_g} (Figure 8c) formulations showed similar R^2 and RMSE of .72 and .011, respectively. All three models had a bias (−0.014 or −0.015 mol m⁻² s⁻¹) and underestimated measured $g_{\text{sw,dark}}$ with the percent underestimation being greater for lower $g_{\text{sw,dark}}$ values. The new model USO_{A_g²}, which was designed to address the nonlinearity between the g_{sw} response variable and the regressor by squaring the numerator in the regressor term lowered the bias in the estimation and made it statistically identical to 0 (Figure 8d). Moreover, in the nonlinear form, the model improved the R^2 of $g_{\text{sw,dark}}$ estimation (Figure 8).

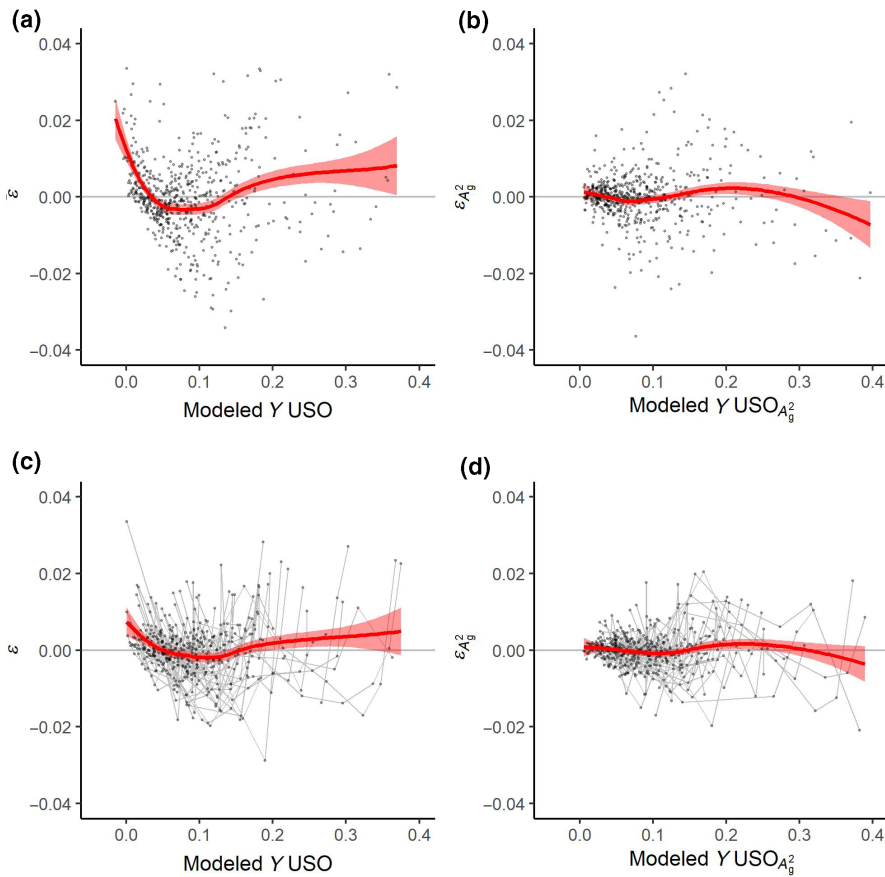


FIGURE 4 Representation of the residuals (ε) of the regression between g_{sw} and the regressor X (Table 2) for the USO and $\text{USO}_{A_g^2}$ models. Panels (a) and (b) correspond to the residuals when only the data acquired at an irradiance over the light compensation point were considered. Panels (c) and (d) correspond to the residuals for an irradiance over $150 \mu\text{mol m}^{-2} \text{s}^{-1}$. The red line presents the trend of the residuals and the shaded area represents the standard error of the mean. For the panels (c) and (d), each gray line represents the residuals of one conductance response curve. The overall trend showed a slight curvilinear trend in panel (c) which was in fact stronger when analysing each curve individually [Colour figure can be viewed at wileyonlinelibrary.com]

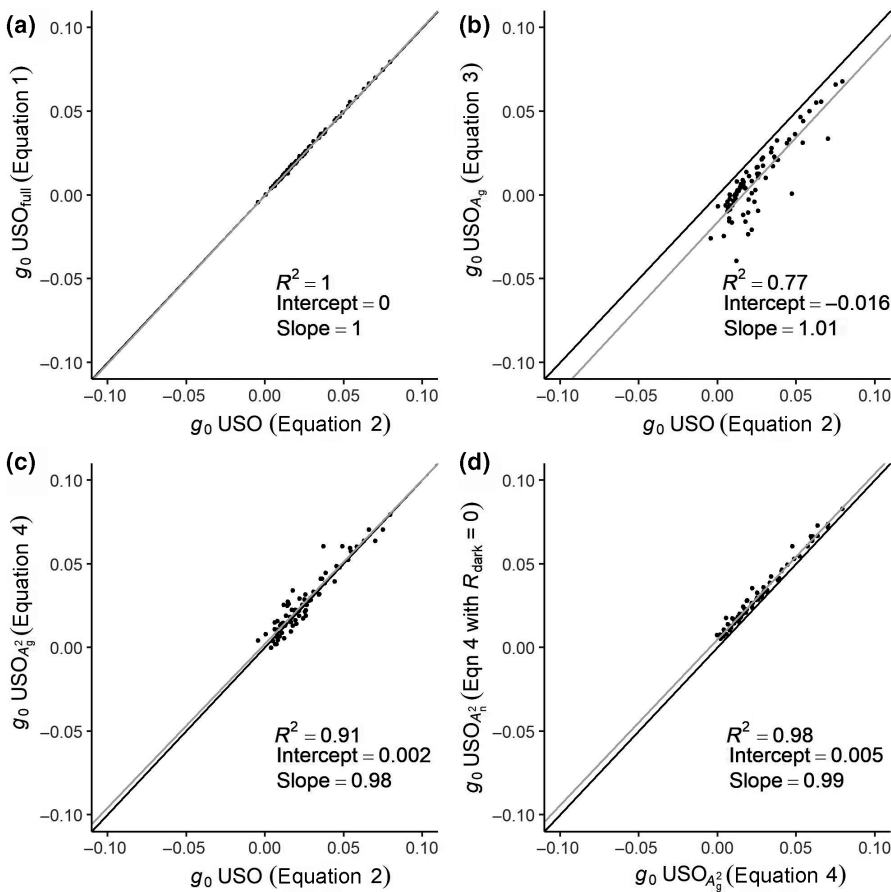


FIGURE 5 Comparison of the values of g_0 estimated using the different conductance models. The gray line corresponds to the linear regression between g_0 estimated by the different models. The slope and intercept of the linear regressions are reported in each panel. The black line corresponds to $y = x$

FIGURE 6 Comparison of the values of g_1 estimated using the different conductance models. The gray line corresponds to the linear regression between g_1 estimated by the different models. The slope and intercept of the linear regressions are reported in each panel

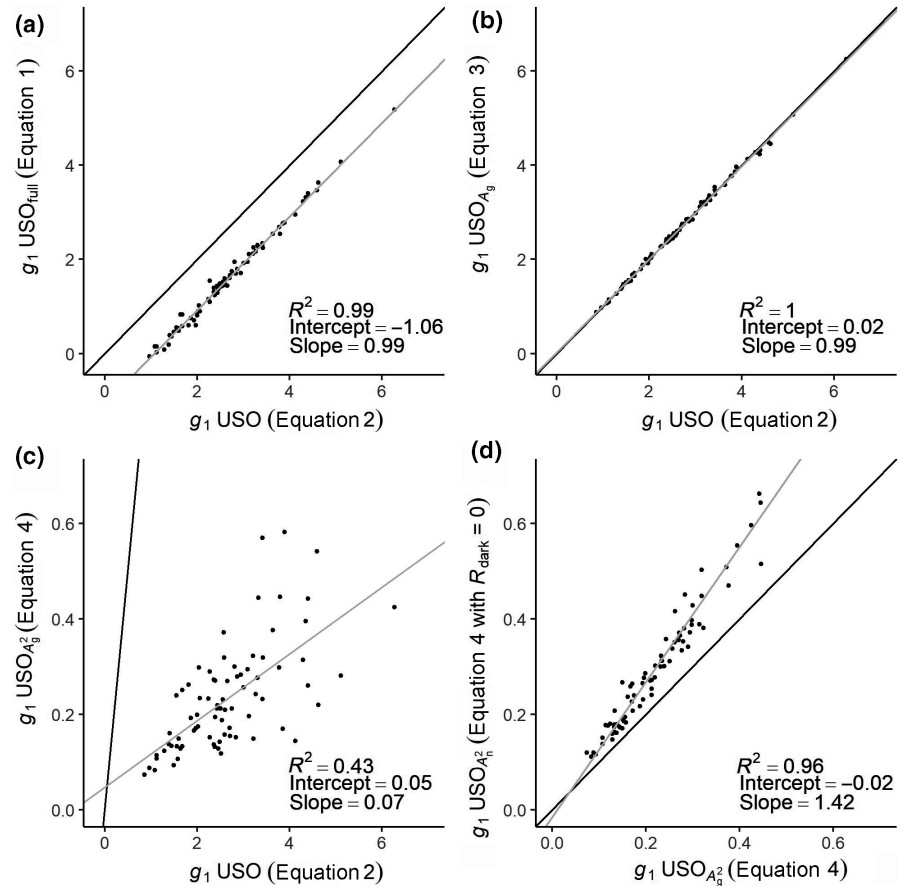


TABLE 3 Analysis of variance of the conductance parameters g_0 and g_1 estimated using the different conductance models USO_{full} , USO , USO_{A_g} and $USO_{A_g^2}$

Parameter	Model	Species				Phenological stage				Residuals		
		df	SSq	F	p	df	SSq	F	p	df	SSq	Adjusted R^2
g_1	USO_{full}	5	34.3	10.3	***	2	4.7	3.5	*	69	45.9	.40
g_1	USO	5	35.1	10.6	***	2	4.3	3.3	*	69	45.6	.41
g_1	USO_{A_g}	5	34.7	10.9	***	2	4.4	3.4	*	69	43.9	.42
g_1	$USO_{A_g^2}$	5	0.49	21	***	2	0.15	15.7	***	69	0.32	.63
g_0	USO_{full}	5	0.003	2.3	ns	2	0.001	2.1	ns	69	0.021	.10
g_0	USO	5	0.003	2.3	ns	2	0.001	2.1	ns	69	0.021	.10
g_0	USO_{A_g}	5	0.006	3.2	*	2	0.001	0.9	ns	69	0.027	.13
g_0	$USO_{A_g^2}$	5	0.005	3.2	*	2	0	0.6	ns	69	0.021	.12

Note: $^{ns}p > .05$; $^*p < .05$; $^{**}p < .01$; $^{***}p < .001$. SSq stands for sum of squares and df stands for degrees of freedom.

3.6 | Performance of the conductance models on independent data sets

First, we tested if the use of the ex situ measurement approach used here and in Leakey et al. (2006) could explain the nonlinearity between g_{sw} and the model regressor. Comparison of the residuals of the USO model on cut and intact branches of hybrid poplar showed that both measurement approaches had the curvilinear trend, clearly demonstrating that the nonlinearity was not attributable to the use

of ex situ measurements (Figure 9a). In addition, VPD_{leaf} was constant within the curves, confirming that the nonlinearity was not caused by this variable. Both the USO and $USO_{A_g^2}$ models had good performance (USO : $R^2 = .93$, $RMSE = 0.018 \text{ mol m}^{-2} \text{ s}^{-1}$; $USO_{A_g^2}$: $R^2 = .96$, $RMSE = 0.015 \text{ mol m}^{-2} \text{ s}^{-1}$, Figure 9a,b), but the trend in the residuals of in situ and ex situ responses was removed by the new $USO_{A_g^2}$ formulation (Figure 9b).

The Leakey et al. (2006) measurements included elevation of CO_{2s} and variation in irradiance. CO_{2s} has a direct effect on

Parameter	Conductance model				
	$V_{\text{cmax}25}$	$R_{\text{dark}25}$	LMA	N_a	
g_1	USO _{full}	-0.06 ^{ns}	-0.12 ^{ns}	-0.09 ^{ns}	-0.20 ^{ns}
g_1	USO	-0.06 ^{ns}	-0.13 ^{ns}	-0.08 ^{ns}	-0.20 ^{ns}
g_1	USO _{A_g}	-0.06 ^{ns}	-0.13 ^{ns}	-0.07 ^{ns}	-0.19 ^{ns}
g_1	USO _{A_g²}	-0.66 ^{***}	-0.35 ^{**}	0.02	-0.43 ^{***}
g_0	USO _{full}	0.01 ^{ns}	-0.09 ^{ns}	0 ^{ns}	0.07 ^{ns}
g_0	USO	0.01 ^{ns}	-0.09 ^{ns}	0 ^{ns}	0.06 ^{ns}
g_0	USO _{A_g}	0.11 ^{ns}	0.25 ^{ns}	0.02 ^{ns}	0.06 ^{ns}
g_0	USO _{A_g²}	0.16 ^{ns}	0.02 ^{ns}	0 ^{ns}	0.16 ^{ns}

Note: ^{ns} $p > .05$; * $p < .05$; ** $p < .01$; *** $p < .001$.

TABLE 4 Leaf trait correlations with g_0 and g_1 estimated by the different conductance models

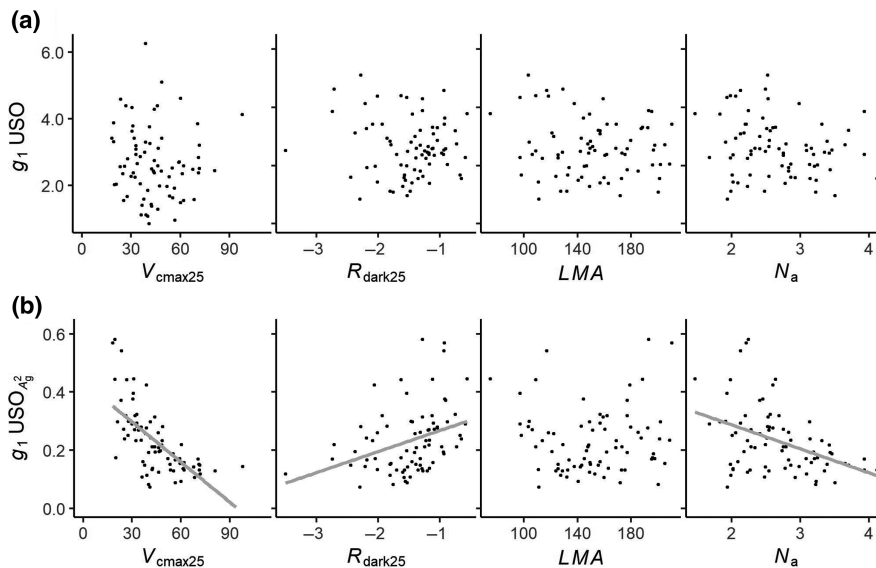


FIGURE 7 F Correlation between the leaf traits and the values of g_1 estimated using the models USO (panel a) and USO_{A_g²} (panel b). The gray line corresponds to the linear regression between the leaf trait and g_1 estimated when the correlation was significant ($p < .01$, Table 4)

estimation of g_{sw} not only because it is present in the denominator of the model equations (Equations 1–4) but also an indirect effect because elevated $\text{CO}_{2\text{s}}$ stimulates A in the numerator (Ainsworth & Rogers, 2007). Squaring the effect of A in USO_{A_g²} could have lowered the ability to model g_{sw} when variation in $\text{CO}_{2\text{s}}$ was considered. However, we saw that the USO_{A_g²} (Figure 9d) had a better performance than the USO (Figure 9c) model ($R^2 = .93$ vs. $R^2 = .86$) and lowered the RMSE by 30% (RMSE = 0.04 vs. RMSE = 0.06). As shown for the data we collected as part of this study, a trend was present in the residuals of the irradiance phase which was removed when using the USO_{A_g²} model (Figure 9c,d).

Similar to the $\text{CO}_{2\text{s}}$ effect, squaring the effect of A in USO_{A_g²} could have lowered the ability to model g_{sw} when variation in T_{leaf} and VPD_{leaf} was considered. For the Lin et al. (2015) global data set, which included a wide range of VPD_{leaf} (between 0.6 and 6 kPa) and T_{leaf} (between 5 and 45°C), both the USO and USO_{A_g²} models had a similar goodness-of-fit. This demonstrated the applicability of the USO_{A_g²} formulation to diverse data collected using the survey approach in a wide range of temperature and VPD_{leaf} (Figure 10a, 10b).

3.7 | Impact of using USO and USO_{A_g²} on leaf gas exchange predictions

The A_n and g_{sw} of an average leaf measured in Panama were simulated for the typical range of irradiance experienced in a photoperiod (0 and 2000 $\mu\text{mol m}^{-2} \text{s}^{-1}$) using the average $V_{\text{cmax}25}$ and $R_{\text{dark}25}$ of all the leaves and the average g_0 and g_1 estimated by the USO and USO_{A_g²} models (Figure 3, all irradiances). Modeled g_{sw} had different values depending on the irradiance (Figure 11a); the two curves crossed at irradiances of 42 and 300 $\mu\text{mol m}^{-2} \text{s}^{-1}$. For low irradiance values, the slope of g_{sw} differed and was lower using the USO_{A_g²} model. At high irradiance, g_{sw} estimated by the USO_{A_g²} model was 21% higher, and this resulted in an increase in intercellular CO_2 concentration and a resulting increase of 7% in A_n . This showed that the choice of the model to fit and simulate the data had an important consequence on modeled A and g_{sw} .

4 | DISCUSSION

Most stomatal models assume that leaf conductance varies linearly with the rate of photosynthesis. This assumption was not supported by

FIGURE 8 Comparison between the conductance measured at $0 \mu\text{mol m}^{-2} \text{s}^{-1}$ irradiance (Observed $g_{\text{sw, dark}}$) and the $g_{\text{sw, dark}}$ modeled using the different conductance formulas (Table 2)

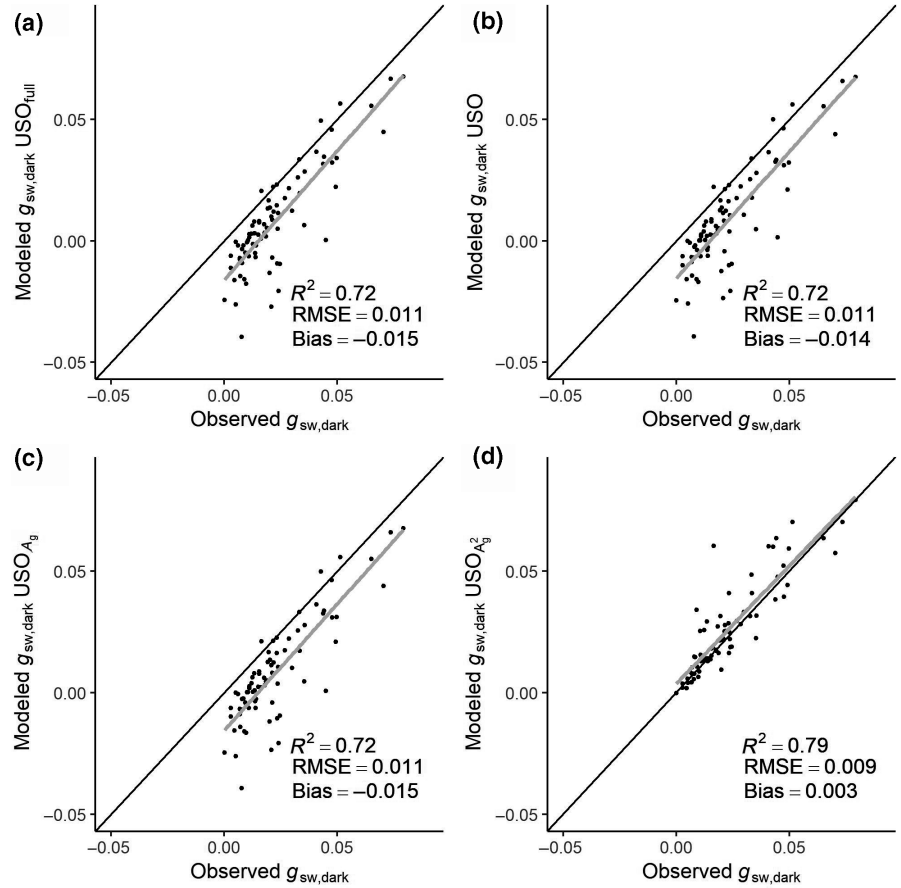
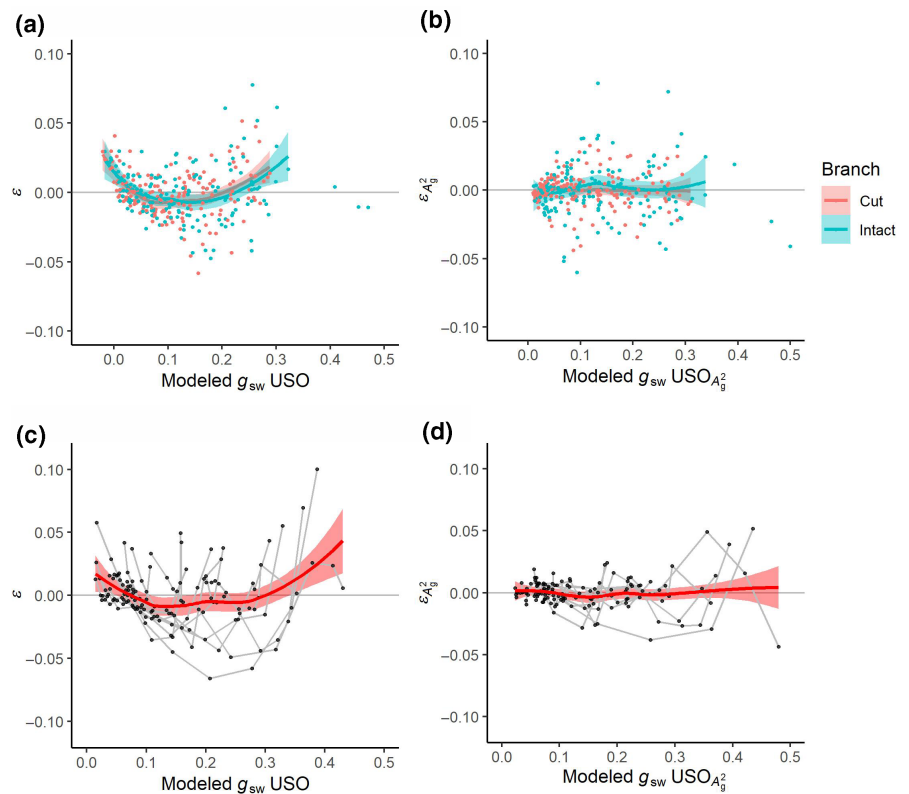


FIGURE 9 Residuals (ϵ) of the USO and $\text{USO}_{A_g^2}$ models for the Davidson et al. (2022) data set measured on cut and intact branches of hybrid poplar (panels a and b) and for the Leakey et al. (2006) data set (panels c and d) for the irradiance phase. For the panels (a) and (b), the three points on the x axis above $0.35 \text{ mol m}^{-2} \text{ s}^{-1}$ were from the same leaf and were not included in the fitting of the trend of the residuals. For the panels (c) and (d), each gray line represents the residuals of one conductance response curve. The overall trend showed a slight curvilinear trend in panel (c), which was in fact stronger when analysing each curve individually [Colour figure can be viewed at wileyonlinelibrary.com]



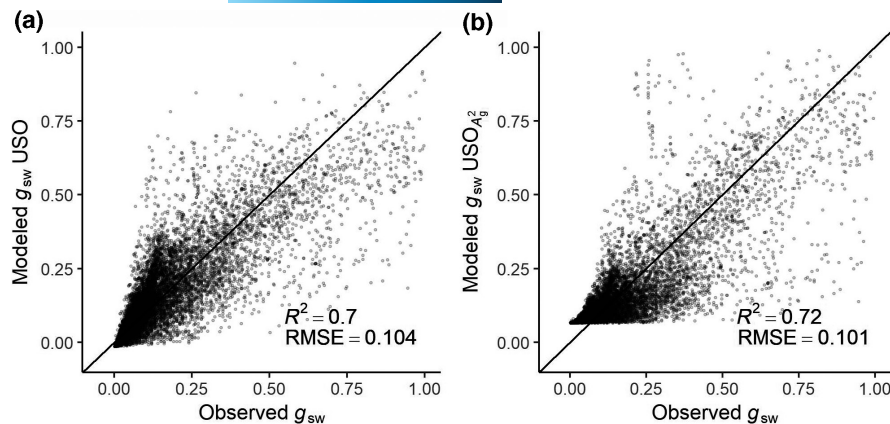


FIGURE 10 Comparison of the goodness-of-fit of the USO and $USO_{A_g^2}$ conductance models on the Lin et al. (2015) data set, which included a large variety of plant species (314), biomes and conditions on the leaf surface with notably a strong variability of T_{leaf} (5.4 and 45.1°C) and VPD_{leaf} (0.6–6 kPa)

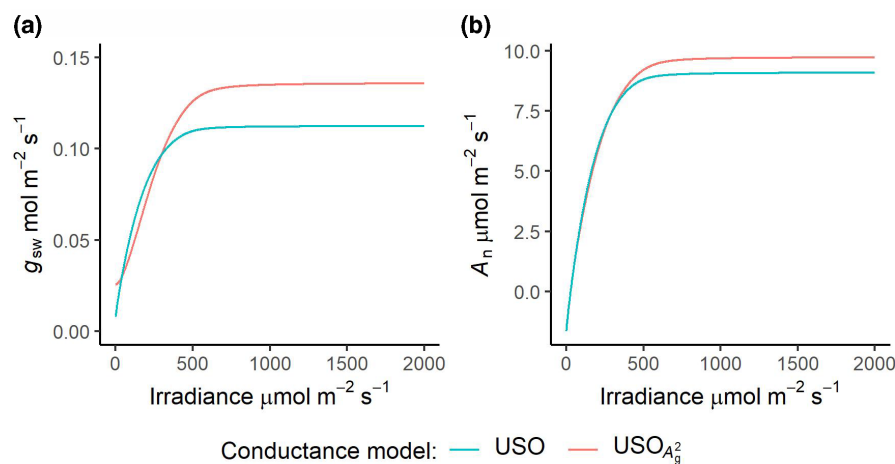


FIGURE 11 Differences in simulation of g_{sw} and A_n made by coupling the conductance models with the Farquhar et al. (1980) photosynthesis model. The parameters used were the average V_{cmax25} and R_{dark25} (54.5 and 1.50 $\mu\text{mol m}^{-2} \text{s}^{-1}$, respectively), and the average g_0 and g_1 estimated by the USO and $USO_{A_g^2}$ models (Figure 3). The input variables T_{leaf} , VPD_{leaf} and CO_{2s} were set constant at 30.1°C, 1.2 kPa, and 400 ppm, respectively, and the light irradiance varied between 0 and 2000 $\mu\text{mol m}^{-2} \text{s}^{-1}$ [Colour figure can be viewed at wileyonlinelibrary.com]

the data. Our observations showed that there is nonlinearity throughout the response, most notably at low and high irradiance (Figures 1, 2 and 4). As a result, estimates of the key stomatal model parameters g_1 and g_0 are highly influenced by the irradiance range of the underlying data used in the parameter estimation which can lead to unreliable and unrealistic parameterization of models and subsequent predictions of g_{sw} and A_n . We have proposed a new empirical formulation that performs well over the full range of irradiance and enables robust estimation of g_1 and g_0 from experimental data. Evaluation with independent data sets demonstrated that this approach works across a range of species, biomes, and with different data collection methods. We also showed that the approach worked whether the change in A was due to changes in irradiance or increases in CO_2 concentration. Furthermore, the new formulation revealed statistically significant correlations between g_1 and other leaf traits that were not identified using g_1 values estimated from current stomatal model formulations, or in our previous work applying the USO model to survey data (Wu et al., 2020).

The USO model was derived from the optimality assumption that stomata respond to ambient conditions so that the marginal cost of water gain (λ) is constant (Cowan & Farquhar, 1977; Medlyn et al., 2011). It was obtained mathematically from biophysical models of leaf photosynthesis and stomatal diffusion and included some simplifying assumptions. Among the simplifying assumptions, it was assumed that the dark respiration is zero and that photosynthesis is limited by the regeneration

of the CO_2 acceptor, ribulose 1,5-bisphosphate (RuBP) and not by the maximum rate of rubisco carboxylation. It is also important to note that the intercept term, g_0 , was not derived by theoretical considerations but was added to respond to empirical evidence that g_{sw} is positive when $A_n = 0$. Under this framework, the points of the regression between g_{sw} and the USO regressor should have had a linear form with the intercept being g_0 and the slope being g_1 (Figure 1). In the data we have evaluated, we have observed that in fact the relationship was nonlinear and that the slope was close to zero when irradiance approached zero and higher for higher values of A . Two hypotheses can be formulated from this result.

First, the optimality hypothesis does not hold and the amount of water that the leaf releases for each mole of CO_2 assimilated is not constant within the typical range of assimilation rates that occur during a day. This hypothesis is supported by previous work which pointed out that the observed positive nocturnal g_{sw} resulted in transpiration without carbon gain (Caird et al., 2007; Yu et al., 2019), therefore challenging the optimality assumption at very low irradiance. We showed in this study that the nonlinearity is also present at irradiances markedly higher than the light compensation point where A_n and g_{sw} values were nearly 40% of their maximum values at saturating irradiance.

However, a second hypothesis could also explain a part of the nonlinearity and is linked to the simplifying assumptions that were made in the USO model. The USO model was derived assuming that

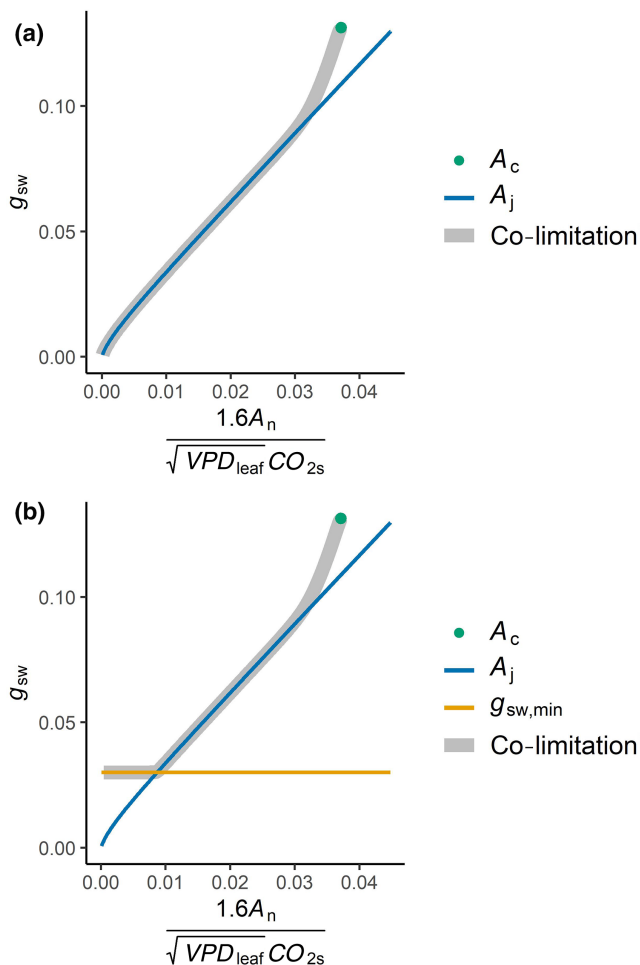


FIGURE 12 (a) Simulation of a conductance response curve using the Buckley et al. (2017) co-limitation optimal model, without (panel a) or with (panel b) the addition of an empirical minimum conductance threshold as suggested by De Kauwe et al. (2015), Lombardozi et al. (2017) and Duursma et al. (2019). In both panels, the point A_c represents the conductance when A is limited by the maximum carboxylation rate of rubisco, the line A_j represents the conductance when A is limited by the maximum rate of RuBP regeneration. A_c limitation corresponds to a point because A_c does not depend on the irradiance. In panel (a), the gray line represents the conductance when A is co-limited by A_c and A_j with a smooth transition between A_c and A_j determined by θ_{c_j} . This gray line corresponds to the model published by Buckley et al. (2017). The nonlinearity at high irradiance (high x ordinate) is due to the transition between A_c and A_j limitations. In panel (b), a minimum limit is added for the conductance and the gray line corresponds to the conductance constrained by 3 limits (A_c , A_j and $g_{sw,min}$). The minimum $g_{sw,min}$ limit explains a nonlinearity at low irradiance for the gray line (low x ordinate) but is not predicted by the Buckley et al. (2017) model and was empirically added here. The parameters used for the simulations in panels a and b were the average V_{cmax25} ($54.5 \mu\text{mol m}^{-2} \text{s}^{-1}$), $J_{max25} = 1.67 V_{cmax25}$, the average R_{dark25} ($1.50 \mu\text{mol m}^{-2} \text{s}^{-1}$), a smoothing factor θ_{c_j} of 0.99 (Buckley et al., 2017) and a λ of $400 \text{ mmol } \mu\text{mol}^{-1}$. For panel b, $g_{sw,min}$ was set to $0.03 \text{ mol m}^{-2} \text{s}^{-1}$. The input variables T_{leaf} , VPD_{leaf} and CO_{2s} were set constant at 30.1°C , 1.2 kPa , and 400 ppm , respectively, and the irradiance varied between 0 and $2000 \mu\text{mol m}^{-2} \text{s}^{-1}$ [Colour figure can be viewed at [wileyonlinelibrary.com](https://onlinelibrary.wiley.com)]

photosynthesis is limited by the rate of RuBP regeneration. This assumption is discussed in detail by Medlyn et al. (2011) and by Huang et al. (2021). This condition is not met when incident irradiance saturates rubisco limited CO_2 assimilation. Buckley et al. (2017) showed that the g_{sw} formulation obtained by optimality models was dependent on the simplifying mathematical assumptions used to derive the equations. They showed that these mathematical assumptions could significantly change g_{sw} predictions and we propose they could account for some elements of the nonlinearity (Figure 12). However, models considering both rubisco limited and RuBP regeneration limited assimilation are less practical to use than the USO model because they require extensive parameterization; V_{cmax25} , J_{max25} , R_{dark25} (as well as their temperature dependence parameters), λ , and a curvature factor associated with the response to irradiance (Buckley et al., 2017), which hinders their application, and is problematic when the USO model is used as a foundation for optimality models that are used to estimate V_{cmax25} (Smith et al., 2019).

A second important assumption in the USO model is the empirical addition of the parameter g_0 to make the conductance higher than 0 when $A_n = 0$. An alternative proposition, which is also empirical, uses the maximum of either a minimum conductance value ($g_{sw,min}$) or $g_1 X$ (Table 2; Figure 12b; Barnard & Bauerle, 2013; De Kauwe et al., 2015; Duursma et al., 2019; Lombardozi et al., 2017). This formulation does a better job at representing the nonlinearity observed in the response to low irradiance but has the disadvantage of only representing the flux associated with minimum conductance—the cuticular conductance and the conductance associated with leaky stomata—at low irradiance. When stomata are actively transpiring and g_{sw} is greater than $g_{sw,min}$, cuticular conductance is ignored. Theoretically, cuticular conductance (represented by a fraction of $g_{sw,min}$) should be always present, whatever the conditions on the leaf surface (Márquez et al., 2021). Note, however, that how to represent the “minimum conductance” in models in an active research area. For example, several studies have shown that g_{sw} responds to stimuli in the dark, such as the concentration of abscisic acid, VPD_{leaf} or CO_2 (Barbour & Buckley, 2007; Caird et al., 2007; Márquez et al., 2021; Resco de Dios et al., 2019; Schreiber, 2001; Zeppel et al., 2012).

Overall, we think that the nonlinearity is likely to be driven by a suboptimal behavior of the leaves that keep a positive g_{sw} in the dark, and maybe by the transition from RuBP limited to Rubisco limited photosynthesis at high light.

Interestingly, a nonlinearity between g_{sw} and A at saturating irradiance ($g_{sw,sat}$ and A_{sat}) was observed in a synthesis of various species with contrasting habitats and life strategies (Deans et al., 2020; Hetherington & Woodward, 2003). This nonlinearity is not currently captured by models that consider optimality attained over longer, life-span scale, integration periods (Deans et al., 2020). The USO model, which seeks to represent the behavior of stomata in response to short-term changes in environmental conditions, functions at a different scale (minutes to hours). However, it is possible

that the same unknown process explains the nonlinearity observed over both short and long timescales.

In this study, we proposed a new empirical g_{sw} model, based on a modification of the Medlyn et al. (2011) formulation. The new model, while based on the USO formulation, is not “optimal” as it was not derived mathematically from an assumption that stomata act to regulate the fluxes of water and CO_2 in an “optimal” way. We recognize that departing from the optimality framework is intellectually unsatisfying as it hinders the interpretability of the parameters of the model since empirical parameters are not grounded in theory (Buckley et al., 2017). We would welcome the development of theoretical formulations that can fully account for the nonlinearity we observed in this study and enable robust parameterization. However, here we show that a key assumption of the USO model (and many other formulations), that is, that the relationship between photosynthesis on g_{sw} is linear, is not supported by observations. Therefore, an empirical formulation that enables robust parameterization has a distinct advantage. Furthermore, in TBMs the modification of derived g_0 and g_1 parameters with empirical scalars undermines a key attraction of the optimality framework (Rogers et al., 2017).

In this study, we have shown that representing the nonlinear effect of A on g_{sw} with a linear relationship added additional uncertainty to simulations of A and g_{sw} and created a consequent bias on the estimation of g_0 and g_1 which was highly dependent on the range of irradiance used in the measurements. The parameter g_0 was smaller when using higher irradiances and became negative using irradiances above $150 \mu\text{mol m}^{-2} \text{s}^{-1}$. The empirical difficulty to estimate g_0 using regressions has been experienced in several studies where negative values were reported (Duursma et al., 2019; Héroult et al., 2013; Leuning, 1995; Medlyn et al., 2011; Miner & Bauerle, 2017). Our results suggest that underestimation of g_0 is likely to result from using a linear model to fit data that are in fact not linear. In contrast, when using the $USO_{A_g^2}$ model, estimation of g_0 was not affected by irradiance and corresponded closely to $g_{sw, \text{dark}}$. In addition, we showed a strong dependence of the range of irradiance on g_1 estimated by the USO model, with higher values when the irradiance, and therefore A , was higher. Note that the bias between g_1 estimated using the full irradiance range, or only the irradiance above $150 \mu\text{mol m}^{-2} \text{s}^{-1}$ (Figure 3b) is significant and results in g_1 values that differ by more than the difference between the g_1 values associated with a tropical rainforest tree and a deciduous savannah tree plant functional type as reported by Lin et al. (2015). Estimating g_1 using the $USO_{A_g^2}$ model improved the robustness of the estimation across the different irradiances. Additionally, we found that g_1 estimated by fitting the data with the $USO_{A_g^2}$ formulation revealed correlation with other leaf traits that were not seen when using g_1 estimated by the USO model. This is an interesting result, and it could lead to a better understanding of trait co-variance that could be used to derive the g_1 parameter from other leaf traits.

We recognize that several formulations could be used to represent the nonlinearity in the g_{sw} response. Initially we evaluated formulations using A_g^k and estimated k for each conductance response curve. We saw that for the various species we studied the mean k was significantly above one ($p < 1.10^{-15}$), with an average around two

($k = 2.1 \pm 0.6$ SD for the tropical species; $k = 1.8 \pm 0.7$ SD for the Davidson et al. (2022) data set; $k = 2.2 \pm 0.6$ SD for the Leakey et al. (2006) data set). However, to avoid overparameterization of the model we chose to fix k to 2. The choice of the representation of the nonlinearity by a power was however strictly empirical, based on the analysis of the residuals, and was not guided by mechanistic insight. Therefore, it is possible that other nonlinear empirical representations could also perform well. It is important to note that even if the modification we propose to the USO model is empirical, the $USO_{A_g^2}$ parameters can still be interpreted within the USO framework. Indeed, g_1 from the USO model is similar to g_1 from the USO_{A_g} model (Equation 3, Figure 6b) and both increased with irradiance (Figure 3). If we consider that g_1 increases proportionally with A_g and, therefore, write $g_1 = cA_g$ in Equation 3, we obtain the $USO_{A_g^2}$ model (Equation 4). Note that we use g_1 in place of c to follow established notation where g_1 is the slope of the conductance model (Table 2).

Our choice of A_g^2 in place of A_n^2 is motivated by the advantage of having $g_0 = g_{sw, \text{dark}}$. In addition, the use of A_n^2 would simulate a slight decrease in g_{sw} with increasing irradiance from dark to the light compensation point, which was not observed in the data. We recognize that A_g is not directly measured by gas exchange instrumentation and that our estimate of A_g is dependent on a dark-adapted measurement of respiration (R_{dark}) that may differ from the respiration in the light (R_{day}) (Atkin et al., 1997; Farquhar & Busch, 2017).

Our study demonstrated the importance of considering the nonlinearity between g_{sw} and A in conductance models for simulating gas exchange but also the influence of this nonlinearity on our ability to provide models with robust parameter estimates. Further studies will be necessary to elucidate the mechanisms involved to explain the nonlinearity and the ecological advantage of this phenomenon. This work focused on the effects of variation in irradiance and considered elevation of ambient CO_2 concentration. Further studies evaluating the non-linearity of the relationship between A and g_{sw} in response to changes in VPD_{leaf} and T_{leaf} would be a valuable addition.

ACKNOWLEDGEMENTS

This work was supported by the Next-Generation Ecosystem Experiments (NGEE Tropics) project that is supported by the Office of Biological and Environmental Research in the Department of Energy, Office of Science, and through the United States Department of Energy Contract No. DE-SC0012704 to Brookhaven National Laboratory. ADBL was supported by Office of Biological and Environmental Research in the DOE Office of Science (DE-SC0018277).

CONFLICT OF INTEREST

The authors declare no competing interests.

AUTHOR CONTRIBUTIONS

Julien Lamour, Kenneth J. Davidson, Shawn P. Serbin, and Alistair Rogers planned and designed the research. Julien Lamour and Kenneth J. Davidson measured the conductance data. Julien Lamour, Kenneth J. Davidson, and Gilles Le Moguédec analyzed the data.

Julien Lamour and Alistair Rogers wrote the manuscript with contributions from Kenneth J. Davidson, Kim S. Ely, Gilles Le Moguédec, Andrew D. B. Leakey, Qianyu Li, and Shawn P. Serbin.

DATA AVAILABILITY STATEMENT

The conductance and leaf traits data that support the findings of this study are publicly available in Julien Lamour, Kenneth Davidson, Kim Ely, Jeremiah Anderson, Alistair Rogers, and Shawn Serbin (2021). Leaf structural and chemical traits, and BNL field campaign sample details, San Lorenzo, Panama, 2020. Ngee Tropics Data Collection. Accessed at <http://dx.doi.org/10.15486/ngt/1783737>.

Julien Lamour, Kenneth Davidson, Kim Ely, Jeremiah Anderson, Shawn Serbin, and Alistair Rogers (2021). Leaf gas exchange and fitted parameters, San Lorenzo, Panama, 2020. Ngee Tropics Data Collection. Accessed at <http://dx.doi.org/10.15486/ngt/1781004>.

CODE AVAILABILITY STATEMENT

The package LeafGasExchange used to simulate Figure 11 is available on Github (Lamour & Serbin, 2021).

ORCID

Julien Lamour  <https://orcid.org/0000-0002-4410-507X>

Kenneth J. Davidson  <https://orcid.org/0000-0001-5745-9689>

Kim S. Ely  <https://orcid.org/0000-0002-3915-001X>

Gilles Le Moguédec  <https://orcid.org/0000-0002-7292-9121>

Andrew D. B. Leakey  <https://orcid.org/0000-0001-6251-024X>

Qianyu Li  <https://orcid.org/0000-0002-0627-039X>

Shawn P. Serbin  <https://orcid.org/0000-0003-4136-8971>

Alistair Rogers  <https://orcid.org/0000-0001-9262-7430>

REFERENCES

- Ainsworth, E. A., & Rogers, A. (2007). The response of photosynthesis and stomatal conductance to rising [CO₂]: Mechanisms and environmental interactions. *Plant, Cell & Environment*, 30(3), 258–270. <https://doi.org/10.1111/j.1365-3040.2007.01641.x>
- Anderegg, W. R. L., Wolf, A., Arango-Velez, A., Choat, B., Chmura, D. J., Jansen, S., Kolb, T., Li, S., Meinzer, F., Pita, P., Resco de Dios, V., Sperry, J. S., Wolfe, B. T., & Pacala, S. (2017). Plant water potential improves prediction of empirical stomatal models. *PLoS One*, 12, e0185481. <https://doi.org/10.1371/journal.pone.0185481>
- Atkin, O. K., Westbeek, M. H. M., Cambridge, M. L., Lambers, H., & Pons, T. L. (1997). Leaf respiration in light and darkness (a comparison of slow- and fast-growing poa species). *Plant Physiology*, 113, 961–965. <https://doi.org/10.1104/pp.113.3.961>
- Ball, J. T. (1988). An analysis of stomatal conductance.
- Ball, J. T., Woodrow, I. E., & Berry, J. A. (1987). A model predicting stomatal conductance and its contribution to the control of photosynthesis under different environmental conditions. In *Progress in photosynthesis research* (pp. 221–224). Springer.
- Barbour, M. M., & Buckley, T. N. (2007). The stomatal response to evaporative demand persists at night in *Ricinus communis* plants with high nocturnal conductance. *Plant, Cell & Environment*, 30, 711–721.
- Barnard, D. M., & Bauerle, W. L. (2013). The implications of minimum stomatal conductance on modeling water flux in forest canopies. *Journal of Geophysical Research: Biogeosciences*, 118, 1322–1333. <https://doi.org/10.1002/jgrg.20112>
- Basset, Y. (2003). *Studying forest canopies from above: The international canopy crane network*. Smithsonian Tropical Research Institute.
- Bonan, G. B., Lawrence, P. J., Oleson, K. W., Levis, S., Jung, M., Reichstein, M., Lawrence, D. M., & Swenson, S. C. (2011). Improving canopy processes in the Community Land Model version 4 (CLM4) using global flux fields empirically inferred from FLUXNET data. *Journal of Geophysical Research*, 116. <https://doi.org/10.1029/2010JG001593>
- Bonan, G. B., Williams, M., Fisher, R. A., & Oleson, K. W. (2014). Modeling stomatal conductance in the earth system: linking leaf water-use efficiency and water transport along the soil–plant–atmosphere continuum. *Geoscientific Model Development*, 7, 2193–2222. <https://doi.org/10.5194/gmd-7-2193-2014>
- Boyer, J. S., Wong, S. C., & Farquhar, G. D. (1997). CO₂ and water vapor exchange across leaf cuticle (epidermis) at various water potentials. *Plant Physiology*, 114, 185–191. <https://doi.org/10.1104/pp.114.1.185>
- Buckley, T. N. (2019). How do stomata respond to water status? *New Phytologist*, 224, 21–36. <https://doi.org/10.1111/nph.15899>
- Buckley, T. N., & Mott, K. A. (2013). Modelling stomatal conductance in response to environmental factors. *Plant, Cell & Environment*, 36, 1691–1699.
- Buckley, T. N., Sack, L., & Farquhar, G. D. (2017). Optimal plant water economy. *Plant, Cell & Environment*, 40, 881–896.
- Burnett, A. C., Davidson, K. J., Serbin, S. P., & Rogers, A. (2019). The “one-point method” for estimating maximum carboxylation capacity of photosynthesis: A cautionary tale. *Plant, Cell & Environment*, 42, 2472–2481. <https://doi.org/10.1111/pce.13574>
- Caird, M. A., Richards, J. H., & Donovan, L. A. (2007). Nighttime stomatal conductance and transpiration in C₃ and C₄ plants. *Plant Physiology*, 143, 4–10. <https://doi.org/10.1104/pp.106.092940>
- Chen, B., Chen, J. M., Baldocchi, D. D., Liu, Y., Wang, S., Zheng, T., Black, T. A., & Croft, H. (2019). Including soil water stress in process-based ecosystem models by scaling down maximum carboxylation rate using accumulated soil water deficit. *Agricultural and Forest Meteorology*, 276–277, 107649. <https://doi.org/10.1016/j.agrfor.2019.107649>
- Clark, D. B., Mercado, L. M., Sitch, S., Jones, C. D., Gedney, N., Best, M. J., Pryor, M., Rooney, G. G., Essery, R. L. H., Blyth, E., Boucher, O., Harding, R. J., Huntingford, C., & Cox, P. M. (2011). The Joint UK Land Environment Simulator (JULES), model description – Part 2: Carbon fluxes and vegetation dynamics. *Geoscientific Model Development*, 4(3), 701–722. <https://doi.org/10.5194/gmd-4-701-2011>
- Cowan, I. R., & Farquhar, G. D. (1977). Stomatal function in relation to leaf metabolism and environment.
- Craine, J. M., & Reich, P. B. (2005). Leaf-level light compensation points in shade-tolerant woody seedlings. *New Phytologist*, 166, 710–713. <https://doi.org/10.1111/j.1469-8137.2005.01420.x>
- Damour, G., Simonneau, T., Cochard, H., & Urban, L. (2010). An overview of models of stomatal conductance at the leaf level. *Plant, Cell & Environment*, 33, 1419–1438.
- Davidson, K. J., Lamour, J., Rogers, A., & Serbin, S. P. (2022). Late day measurement of excised branches results in uncertainty in the estimation of two stomatal parameters derived from response curves in *Populus deltoides* Bartr. X *Populus nigra* L. *Tree Physiology*, tpac006. <https://doi.org/10.1093/treephys/tpac006>
- De Kauwe, M. G., Kala, J., Lin, Y.-S., Pitman, A. J., Medlyn, B. E., Duursma, R. A., Abramowitz, G., Wang, Y.-P., & Miralles, D. G. (2015). A test of an optimal stomatal conductance scheme within the CABLE land surface model. *Geoscientific Model Development*, 8, 431–452. <https://doi.org/10.5194/gmd-8-431-2015>
- De Kauwe, M. G., Lin, Y.-S., Wright, I. J., Medlyn, B. E., Crous, K. Y., Ellsworth, D. S., Maire, V., Prentice, I. C., Atkin, O. K., Rogers, A., Niinemets, Ü., Serbin, S. P., Meir, P., Uddling, J., Togashi, H. F., Tarvainen, L., Weerasinghe, L. K., Evans, B. J., Ishida, F. Y., & Domingues, T. F. (2016). A test of the ‘one-point method’ for estimating maximum carboxylation capacity from field-measured,

- light-saturated photosynthesis. *New Phytologist*, 210(3), 1130–1144. <https://doi.org/10.1111/nph.13815>
- Deans, R. M., Brodribb, T. J., Busch, F. A., & Farquhar, G. D. (2020). Optimization can provide the fundamental link between leaf photosynthesis, gas exchange and water relations. *Nature Plants*, 6, 1116–1125.
- Dietze, M. C., Serbin, S. P., Davidson, C., Desai, A. R., Feng, X., Kelly, R., Kooper, R., LeBauer, D., Mantooh, J., McHenry, K., & Wang, D. (2014). A quantitative assessment of a terrestrial biosphere model's data needs across North American biomes. *Journal of Geophysical Research: Biogeosciences*, 119, 286–300. <https://doi.org/10.1002/2013JG002392>
- Domingues, T. F., Martinelli, L. A., & Ehleringer, J. R. (2014). Seasonal patterns of leaf-level photosynthetic gas exchange in an eastern Amazonian rain forest. *Plant Ecology & Diversity*, 7, 189–203. <https://doi.org/10.1080/17550874.2012.748849>
- Duursma, R. A., Blackman, C. J., Lopéz, R., Martin-StPaul, N. K., Cochard, H., & Medlyn, B. E. (2019). On the minimum leaf conductance: Its role in models of plant water use, and ecological and environmental controls. *New Phytologist*, 221, 693–705.
- Farquhar, G. D., & Busch, F. A. (2017). Changes in the chloroplastic CO₂ concentration explain much of the observed Kok effect: A model. *New Phytologist*, 214, 570–584.
- Farquhar, G. D., von Caemmerer, S., & Berry, J. A. (1980). A biochemical model of photosynthetic CO₂ assimilation in leaves of C₃ species. *Planta*, 149, 78–90. <https://doi.org/10.1007/BF00386231>
- Fauset, S., Oliveira, L., Buckeridge, M. S., Foyer, C. H., Galbraith, D., Tiwari, R., & Gloor, M. (2019). Contrasting responses of stomatal conductance and photosynthetic capacity to warming and elevated CO₂ in the tropical tree species *Alchornea glandulosa* under heat-wave conditions. *Environmental and Experimental Botany*, 158, 28–39. <https://doi.org/10.1016/j.envexpbot.2018.10.030>
- Franks, P. J., Berry, J. A., Lombardozi, D. L., & Bonan, G. B. (2017). Stomatal function across temporal and spatial scales: Deep-time trends, land-atmosphere coupling and global models. *Plant Physiology*, 174, 583–602.
- Franks, P. J., Bonan, G. B., Berry, J. A., Lombardozi, D. L., Holbrook, N. M., Herold, N., & Oleson, K. W. (2018). Comparing optimal and empirical stomatal conductance models for application in Earth system models. *Global Change Biology*, 24, 5708–5723. <https://doi.org/10.1111/gcb.14445>
- Ghimire, C. P., Bruijnzeel, L. A., Lubczynski, M. W., Zwartendijk, B. W., Odongo, V. O., Ravelona, M., van Meerveld, H. J. (2018). Transpiration and stomatal conductance in a young secondary tropical montane forest: contrasts between native trees and invasive understorey shrubs. *Tree Physiology*, 38, 1053–1070. <https://doi.org/10.1093/treephys/tpy004>
- Hérault, A., Lin, Y.-S., Bourne, A., Medlyn, B. E., & Ellsworth, D. S. (2013). Optimal stomatal conductance in relation to photosynthesis in climatically contrasting Eucalyptus species under drought. *Plant, Cell & Environment*, 36, 262–274.
- Heskel, M. A., O'Sullivan, O. S., Reich, P. B., Tjoelker, M. G., Weerasinghe, L. K., Penillard, A., Egerton, J. J. G., Creek, D., Bloomfield, K. J., Xiang, J., Sinca, F., Stangl, Z. R., Martinez-de la Torre, A., Griffin, K. L., Huntingford, C., Hurry, V., Meir, P., Turnbull, M. H., & Atkin, O. K. (2016). Convergence in the temperature response of leaf respiration across biomes and plant functional types. *Proceedings of the National Academy of Sciences of the United States of America*, 113, 3832–3837. <https://doi.org/10.1073/pnas.1520282113>
- Hetherington, A. M., & Woodward, F. I. (2003). The role of stomata in sensing and driving environmental change. *Nature*, 424, 901–908. <https://doi.org/10.1038/nature01843>
- Huang, G., Yang, Y., Zhu, L., Peng, S., & Li, Y. (2021). Temperature responses of photosynthesis and stomatal conductance in rice and wheat plants. *Agricultural and Forest Meteorology*, 300, 108322. <https://doi.org/10.1016/j.agrformet.2021.108322>
- Körner, C. H. (1995). Leaf diffusive conductances in the major vegetation types of the globe. In E.-D. Schulze & M. M. Caldwell (Eds). *Ecophysiology of photosynthesis* (pp. 463–490). Springer Berlin Heidelberg.
- Krinner, G., Viovy, N., de Noblet-Ducoudré, N., Ogée, J., Polcher, J., Friedlingstein, P., Ciais, P., Sitch, S., & Prentice, I. C. (2005). A dynamic global vegetation model for studies of the coupled atmosphere-biosphere system. *Global Biogeochemical Cycles*, 19. <https://doi.org/10.1029/2003GB002199>
- Kromdijk, J., Głowacka, K., & Long, S. P. (2019). Predicting light-induced stomatal movements based on the redox state of plastoquinone: Theory and validation. *Photosynthesis Research*, 141, 83–97. <https://doi.org/10.1007/s11120-019-00632-x>
- Kumarathunge, D. P., Medlyn, B. E., Drake, J. E., Tjoelker, M. G., Aspinwall, M. J., Battaglia, M., Cano, F. J., Carter, K. R., Cavaleri, M. A., Cernusak, L. A., Chambers, J. Q., Crous, K. Y., De Kauwe, M. G., Dillaway, D. N., Dreyer, E., Ellsworth, D. S., Ghannoum, O., Han, Q., Hikosaka, K., ... Way, D. A. (2019). Acclimation and adaptation components of the temperature dependence of plant photosynthesis at the global scale. *New Phytologist*, 222, 768–784. <https://doi.org/10.1111/nph.15668>
- Lamour, J., & Serbin, S. P. (2021). LeafGasExchange: An R package for fitting and simulating leaf level gas exchange.
- Leakey, A. D. B., Bernacchi, C. J., Ort, D. R., & Long, S. P. (2006). Long-term growth of soybean at elevated [CO₂] does not cause acclimation of stomatal conductance under fully open-air conditions. *Plant, Cell & Environment*, 29, 1794–1800. <https://doi.org/10.1111/j.1365-3040.2006.01556.x>
- Leuning, R. (1995). A critical appraisal of a combined stomatal-photosynthesis model for C₃ plants. *Plant, Cell & Environment*, 18, 339–355. <https://doi.org/10.1111/j.1365-3040.1995.tb00370.x>
- Lin, Y.-S., Medlyn, B. E., Duursma, R. A., Prentice, I. C., Wang, H., Baig, S., Eamus, D., de Dios, V. R., Mitchell, P., Ellsworth, D. S., de Beeck, M. O., Wallin, G., Uddling, J., Tarvainen, L., Linderson, M.-L., Cernusak, L. A., Nippert, J. B., Ocheltree, T. W., Tissue, D. T., ... Wingate, L. (2015). Optimal stomatal behaviour around the world. *Nature Climate Change*, 5, 459–464. <https://doi.org/10.1038/nclimate2550>
- Lombardozi, D. L., Zeppel, M. J. B., Fisher, R. A., & Tawfik, A. (2017). Representing nighttime and minimum conductance in CLM4.5: Global hydrology and carbon sensitivity analysis using observational constraints. *Geoscientific Model Development*, 10, 321–331. <https://doi.org/10.5194/gmd-10-321-2017>
- Machado, R., Loram-Lourenço, L., Farnese, F. S., Alves, R. D. F. B., de Sousa, L. F., Silva, F. G., Filho, S. C. V., Torres-Ruiz, J. M., Cochard, H., & Menezes-Silva, P. E. (2021). Where do leaf water leaks come from? Trade-offs underlying the variability in minimum conductance across tropical savanna species with contrasting growth strategies. *New Phytologist*, 229, 1415–1430. <https://doi.org/10.1111/nph.16941>
- Márquez, D. A., Stuart-Williams, H., & Farquhar, G. D. (2021). An improved theory for calculating leaf gas exchange more precisely accounting for small fluxes. *Nature Plants*, 7, 317–326. <https://doi.org/10.1038/s41477-021-00861-w>
- Medlyn, B. E., Dreyer, E., Ellsworth, D., Forstreuter, M., Harley, P. C., Kirschbaum, M. U. F., Le Roux, X., Montpied, P., Strassmeyer, J., Walcroft, A., Wang, K., & Loustau, D. (2002). Temperature response of parameters of a biochemically based model of photosynthesis. II. A review of experimental data. *Plant, Cell & Environment*, 25(9), 1167–1179. <https://doi.org/10.1046/j.1365-3040.2002.00891.x>
- Medlyn, B. E., Duursma, R. A., Eamus, D., Ellsworth, D. S., Prentice, I. C., Barton, C. V. M., Crous, K. Y., Angelis, P. D., Freeman, M., & Wingate, L. (2011). Reconciling the optimal and empirical approaches to modelling stomatal conductance. *Global Change Biology*, 17, 2134–2144. <https://doi.org/10.1111/j.1365-2486.2010.02375.x>

- Migliavacca, M., Musavi, T., Mahecha, M. D., Nelson, J. A., Knauer, J., Baldocchi, D. D., Perez-Priego, O., Christiansen, R., Peters, J., Anderson, K., Michael Bahn, T., Black, A., Blanken, P. D., Bonal, D., Buchmann, N., Caldararu, S., Carrara, A., Carvalhais, N., Cescatti, A., ... Ikawa, H. (2021). The three major axes of terrestrial ecosystem function. *Nature*, 598, 468–472.
- Miner, G. L., & Bauerle, W. L. (2017). Seasonal variability of the parameters of the Ball-Berry model of stomatal conductance in maize (*Zea mays* L.) and sunflower (*Helianthus annuus* L.) under well-watered and water-stressed conditions. *Plant, Cell & Environment*, 40, 1874–1886.
- Miner, G. L., Bauerle, W. L., & Baldocchi, D. D. (2017). Estimating the sensitivity of stomatal conductance to photosynthesis: A review. *Plant, Cell & Environment*, 40, 1214–1238. <https://doi.org/10.1111/pce.12871>
- Motzer, T., Munz, N., Küppers, M., Schmitt, D., & Anhof, D. (2005). Stomatal conductance, transpiration and sap flow of tropical montane rain forest trees in the southern Ecuadorian Andes. *Tree Physiology*, 25, 1283–1293.
- Ono, K., Maruyama, A., Kuwagata, T., Mano, M., Takimoto, T., Hayashi, K., Hasegawa, T., & Miyata, A. (2013). Canopy-scale relationships between stomatal conductance and photosynthesis in irrigated rice. *Global Change Biology*, 19, 2209–2220. <https://doi.org/10.1111/gcb.12188>
- Osnas, J. L. D., Katabuchi, M., Kitajima, K., Wright, S. J., Reich, P. B., Van Bael, S. A., Kraft, N. J. B., Samaniego, M. J., Pacala, S. W., & Lichstein, J. W. (2018). Divergent drivers of leaf trait variation within species, among species, and among functional groups. *Proceedings of the National Academy of Sciences of the United States of America*, 115, 5480–5485.
- R Core Team. (2020). *R: A language and environment for statistical computing*. R Foundation for Statistical Computing.
- Resco de Dios, V., Chowdhury, F. I., Granda, E., Yao, Y., & Tissue, D. T. (2019). Assessing the potential functions of nocturnal stomatal conductance in C₃ and C₄ plants. *New Phytologist*, 223, 1696–1706.
- Rogers, A., Medlyn, B. E., Dukes, J. S., Bonan, G., Caemmerer, S., Dietze, M. C., Kattge, J., Leakey, A. D. B., Mercado, L. M., Niinemets, Ü., Prentice, I. C., Serbin, S. P., Sitch, S., Way, D. A., & Zaehle, S. (2017). A roadmap for improving the representation of photosynthesis in Earth system models. *New Phytologist*, 213, 22–42. <https://doi.org/10.1111/nph.14283>
- Saito, K., & Futakuchi, K. (2010). Genotypic variation in epidermal conductance and its associated traits among *Oryza sativa* and *O. glaberrima* cultivars and their interspecific progenies. *Crop Science*, 50, 227–234.
- Schreiber, L. (2001). Effect of temperature on cuticular transpiration of isolated cuticular membranes and leaf discs. *Journal of Experimental Botany*, 52, 1893–1900. <https://doi.org/10.1093/jxb/52.362.1893>
- Sellers, P. J., Dickinson, R. E., Randall, D. A., Betts, A. K., Hall, F. G., Berry, J. A., Collatz, G. J., Denning, A. S., Mooney, H. A., Nobre, C. A., Sato, N., Field, C. B., & Henderson-Sellers, A. (1997). Modeling the exchanges of energy, water, and carbon between continents and the atmosphere. *Science*, 275(5299), 502–509. <https://doi.org/10.1126/science.275.5299.502>
- Slot, M., & Winter, K. (2017). In situ temperature response of photosynthesis of 42 tree and liana species in the canopy of two Panamanian lowland tropical forests with contrasting rainfall regimes. *New Phytologist*, 214, 1103–1117.
- Smith, N. G., Keenan, T. F., Colin Prentice, I., Wang, H., Wright, I. J., Niinemets, Ü., Crous, K. Y., Domingues, T. F., Guerrieri, R., Yoko Ishida, F., Kattge, J., Kruger, E. L., Maire, V., Rogers, A., Serbin, S. P., Tarvainen, L., Togashi, H. F., Townsend, P. A., Wang, M., ... Zhou, S.-X. (2019). Global photosynthetic capacity is optimized to the environment. *Ecology Letters*, 22, 506–517. <https://doi.org/10.1111/ele.13210>
- Sperry, J. (2013). Cutting-edge research or cutting-edge artefact? An overdue control experiment complicates the xylem refilling story. *Plant, Cell & Environment*, 36, 1916–1918.
- Sterck, F. J., Duursma, R. A., Pearcy, R. W., Valladares, F., Cieslak, M., & Weemstra, M. (2013). Plasticity influencing the light compensation point offsets the specialization for light niches across shrub species in a tropical forest understorey. *Journal of Ecology*, 101, 971–980. <https://doi.org/10.1111/1365-2745.12076>
- Tuzet, A., Perrier, A., & Leuning, R. (2003). A coupled model of stomatal conductance, photosynthesis and transpiration. *Plant, Cell & Environment*, 26, 1097–1116.
- Wolz, K. J., Wertin, T. M., Abordo, M., Wang, D., & Leakey, A. D. B. (2017). Diversity in stomatal function is integral to modelling plant carbon and water fluxes. *Nature Ecology & Evolution*, 1, 1292–1298. <https://doi.org/10.1038/s41559-017-0238-z>
- Wu, J., Chavana-Bryant, C., Prohaska, N., Serbin, S. P., Guan, K., Albert, L. P., Yang, X., van Leeuwen, W. J. D., Garnello, A. J., Martins, G., Malhi, Y., Gerard, F., Oliveira, R. C., & Saleska, S. R. (2017). Convergence in relationships between leaf traits, spectra and age across diverse canopy environments and two contrasting tropical forests. *New Phytologist*, 214(3), 1033–1048. <https://doi.org/10.1111/nph.14051>
- Wu, J., Serbin, S. P., Ely, K. S., Wolfe, B. T., Dickman, L. T., Grossiord, C., Michaletz, S. T., Collins, A. D., Detto, M., McDowell, N. G., Wright, S. J., & Rogers, A. (2020). The response of stomatal conductance to seasonal drought in tropical forests. *Global Change Biology*, 26, 823–839. <https://doi.org/10.1111/gcb.14820>
- Xu, L., & Baldocchi, D. D. (2003). Seasonal trends in photosynthetic parameters and stomatal conductance of blue oak (*Quercus douglasii*) under prolonged summer drought and high temperature. *Tree Physiology*, 23, 865–877. <https://doi.org/10.1093/treephys/23.13.865>
- Yin, X., & Struik, P. C. (2009). C₃ and C₄ photosynthesis models: An overview from the perspective of crop modelling. *NJAS - Wageningen Journal of Life Sciences*, 57, 27–38.
- Yu, K., Goldsmith, G. R., Wang, Y., & Anderegg, W. R. L. (2019). Phylogenetic and biogeographic controls of plant nighttime stomatal conductance. *New Phytologist*, 222, 1778–1788. <https://doi.org/10.1111/nph.15755>
- Zeppel, M. J. B., Lewis, J. D., Chazsar, B., Smith, R. A., Medlyn, B. E., Huxman, T. E., & Tissue, D. T. (2012). Nocturnal stomatal conductance responses to rising [CO₂], temperature and drought. *New Phytologist*, 193, 929–938.
- Zhou, S., Duursma, R. A., Medlyn, B. E., Kelly, J. W. G., & Prentice, I. C. (2013). How should we model plant responses to drought? An analysis of stomatal and non-stomatal responses to water stress. *Agricultural and Forest Meteorology*, 182–183, 204–214. <https://doi.org/10.1016/j.agrformet.2013.05.009>
- Zhu, G.-F., Li, X., Su, Y.-H., Lu, L., Huang, C.-L., & Niinemets, Ü. (2011). Seasonal fluctuations and temperature dependence in photosynthetic parameters and stomatal conductance at the leaf scale of *Populus euphratica* Oliv. *Tree Physiology*, 31, 178–195.

SUPPORTING INFORMATION

Additional supporting information may be found in the online version of the article at the publisher's website.

How to cite this article: Lamour, J., Davidson, K. J., Ely, K. S., Le Moguédec, G., Leakey, A. D. B., Li, Q., Serbin, S. P., & Rogers, A. (2022). An improved representation of the relationship between photosynthesis and stomatal conductance leads to more stable estimation of conductance parameters and improves the goodness-of-fit across diverse data sets. *Global Change Biology*, 28, 3537–3556. <https://doi.org/10.1111/gcb.16103>

APPENDIX

The equations used to simulate the leaf gas exchange (Figure 10) are presented below.

We used the FCB photosynthesis model (Farquhar et al., 1980), which represents net CO₂ assimilation rate as:

$$A_n = \min(A_c, A_j) - R_d, \quad (A1)$$

where A_c is the rate of maximum carboxylation and A_j is the maximum rate of RuBp regeneration (or electron transport) and R_d is the daytime respiration rate that is not attributable to the photorespiratory pathway.

A_c and A_j are given by:

$$A_c = \frac{(C_i - \Gamma^*) V_{cmax}}{C_i + K_c \left(1 + \frac{O_2}{K_o}\right)}, \quad (A2)$$

$$A_j = \frac{(C_i - \Gamma^*) \frac{J}{4}}{C_i + 2\Gamma^*}, \quad (A3)$$

where Γ^* is photorespiratory CO₂ compensation point, C_i is the intercellular CO₂ concentration, V_{cmax} is the maximum carboxylation velocity, K_c and K_o are the Michaelis-Menten coefficients of rubisco activity for CO₂ and O₂, respectively, and J is the potential electron transport rate, given by:

$$J = \frac{I_2 + J_{max} - \sqrt{(I_2 + J_{max})^2 - 4\theta I_2 J_{max}}}{2\theta}, \quad (A4)$$

where I_2 is the photosynthetic irradiance absorbed by the photosystem II, J_{max} is the maximum electron transport rate and θ is an empirical curvature factor (usually around 0.7).

Note that Equations (A2) and (A3) are in the form:

$$A_n = \frac{(C_i - \Gamma^*) x}{C_i + y} - R_d, \quad (A5)$$

where x and y equal V_{cmax} and $K_c \left(1 + \frac{O_2}{K_o}\right)$, respectively, when A_n is limited by A_c , and equal $J/4$ and $2\Gamma^*$, respectively, when A_n is limited by A_j .

The diffusion of the CO₂ from the leaf surface to the intercellular environment can be described by:

$$C_i = CO_{2s} - 1.6 \frac{A_n}{g_{sw}}. \quad (A6)$$

And finally, the leaf conductance to water vapor is modeled using the USO_{A₂} model:

$$g_{sw} = g_0 + 1.6 \frac{g_1}{\sqrt{VPD_{leaf}}} \frac{A_g^2}{CO_{2s}}, \quad (A7)$$

where $A_g = A_n + R_d$.

We assumed that R_d corresponds to respiration in the dark (R_{dark}).

In those conditions, the solutions of the system of equations {Equations A5-A7} for C_i corresponds to the roots of a degree 3 polynomial (below). In our simulations, among the three solutions two were imaginary and one was real. The real solution was used and was then used to calculate A_n and g_{sw} :

$$aC_i^3 + bC_i^2 + cC_i + d = 0, \quad (A8)$$

where:

$$a = 5g_0CO_{2s}\sqrt{VPD_{leaf}} + 8g_1x^2,$$

$$b = -16\Gamma^*g_1x^2 - 5\sqrt{VPD_{leaf}}CO_{2s}^2g_0 + 10\sqrt{VPD_{leaf}}CO_{2s}g_0y - 8CO_{2s}g_1x^2 - 8\sqrt{VPD_{leaf}}R_{dark}CO_{2s} + 8\sqrt{VPD_{leaf}}CO_{2s}x,$$

$$c = 8\Gamma^{*2}g_1x^2 + 16\Gamma^*CO_{2s}g_1x^2 - 10\sqrt{VPD_{leaf}}CO_{2s}^2g_0y + 5\sqrt{VPD_{leaf}}CO_{2s}g_0y^2 - 8\Gamma^*\sqrt{VPD_{leaf}}CO_{2s}x - 16\sqrt{VPD_{leaf}}R_{dark}CO_{2s}y + 8\sqrt{VPD_{leaf}}CO_{2s}xy,$$

$$d = -8\Gamma^{*2}CO_{2s}g_1x^2 - 5\sqrt{VPD_{leaf}}CO_{2s}^2g_0y^2 - 8\Gamma^*\sqrt{VPD_{leaf}}CO_{2s}xy - 8\sqrt{VPD_{leaf}}R_{dark}CO_{2s}y^2.$$